CANCER

Immunity drives *TET1* regulation in cancer through NF-κB

Evelyne Collignon[1]*, Annalisa Canale[2]*, Clémence Al Wardi[1], Martin Bizet[1], Emilie Calonne[1], Sarah Dedeurwaerder[1], Soizic Garaud[3], Céline Naveaux[3], Whitney Barham[4], Andrew Wilson[4], Sophie Bouchat[5], Pascale Hubert[6], Carine Van Lint[5], Fiona Yull[4], Christos Sotiriou[7], Karen Willard-Gallo[3], Agnès Noel[2]†, François Fuks[1]†

Ten-eleven translocation enzymes (TET1, TET2, and TET3), which induce DNA demethylation and gene regulation by converting 5-methylcytosine (5mC) to 5-hydroxymethylcytosine (5hmC), are often down-regulated in cancer. We uncover, in basal-like breast cancer (BLBC), genome-wide 5hmC changes related to *TET1* regulation. We further demonstrate that *TET1* repression is associated with high expression of immune markers and high infiltration by immune cells. We identify in BLBC tissues an anticorrelation between *TET1* expression and the major immunoregulator family nuclear factor κB (NF-κB). In vitro and in mice, *TET1* is down-regulated in breast cancer cells upon NF-κB activation through binding of p65 to its consensus sequence in the *TET1* promoter. We lastly show that these findings extend to other cancer types, including melanoma, lung, and thyroid cancers. Together, our data suggest a novel mode of regulation for *TET1* in cancer and highlight a new paradigm in which the immune system can influence cancer cell epigenetics.

INTRODUCTION

Breast cancer (BC) is a very heterogeneous disease characterized by different molecular and histopathological features, responses to therapy, and patient outcomes (*1*). This complexity has prompted researchers and clinicians to stratify breast tumors. Gene expression profiling has identified four main subtypes of BC (*2*, *3*). Luminal A BCs express the estrogen receptor (ER) and/or the progesterone receptor (PR) and have a good prognosis. Luminal B tumors are also ER^+/PR^+ but are associated with a worse prognosis. HER2-like tumors are characterized by amplification of the *Erbb2* (*HER2*) gene, are high grade, and have a poor prognosis. Basal-like BCs (BLBCs) are generally negative for the three receptors (that is, $ER^-/PR^-/HER2^-$ or "triple negative") and are associated with a poor outcome (*4*–*6*).

In recent years, epigenetic features have emerged as major characteristics of cancers. Epigenetic modifications interfere with gene expression, and abnormal epigenetic modification patterns are involved in cancer development and progression (*7*). In this regard, the discovery of DNA cytosine hydroxymethylation is of great interest (*8*, *9*). Ten-eleven translocation enzymes (TET1, TET2, and TET3) catalyze the oxidation of 5-methylcytosine (5mC) to 5-hydroxymethylcytosine (5hmC) (*10*, *11*), leading to DNA demethylation and gene regulation (*12*–*15*). Global loss of 5hmC, associated with *TET* down-regulation and/or alteration of TET functions, has been described as a hallmark of cancer. This dysregulation has been described in both hematological and solid tumors, including colon, liver, lung, skin (melanoma), prostate, and breast tumors (*16*–*19*). In mammary tumors, *TET1* especially has been described as a tumor suppressor gene, and its reduced expression appears to promote cancer growth and metastasis (*18*, *20*–*22*). In BC and other solid tumors, *TET1* is rarely mutated, but its activity is affected by several mechanisms, such as down-regulation by MiR-29 or HMGA2 or through promoter methylation (*12*, *18*, *20*–*24*). Despite growing knowledge, much remains to be learned about the regulation of TET enzymes and notably about their relationship with central signaling pathways involved in cancer.

A greater attention has recently focused on the complex but essential role of immune responses in cancer. An immune response can either repress tumor development and progression (for example, through immunosurveillance and the destruction of tumor cells) or promote it (for example, through secretion of protumorigenic and proinflammatory factors) (*25*). The prognostic and predictive value of tumor-infiltrating lymphocytes (TILs) in many cancer types (*26*–*28*) and the recent emergence of immunotherapy in clinical oncology (*29*) notably illustrate the importance of the immune system in cancer.

Among the immune signaling pathways, the nuclear factor κB (NF-κB) pathway is commonly activated in cancer. NF-κB, composed of five members, p65 (RelA), RelB, c-Rel, NF-κB1, and NF-κB2, was first identified as a transcription factor crucial to the development, survival, and activation of leukocytes (including B and T lymphocytes) and macrophages (*30*). It is known to be involved not only in gene expression, acting either as a transcriptional activator or repressor (*31*–*33*), but also for its interactions with other key immune pathways, such as STAT3 (signal transducer and activator of transcription 3) signaling, which makes it a central regulator of immune signaling (*34*–*36*). In addition, NF-κB is a central pathway in the mammary gland, where it regulates epithelial proliferation and branching during early development, and is frequently activated in BC, particularly in the BLBC subtype (*37*–*40*). The role of NF-κB proteins in cancer is complex. Generally viewed as protumorigenic, they are involved in cell survival, invasion, angiogenesis, metastasis, and chemoresistance (*41*–*45*). However, several reports suggest that they might also oppose cancer development (*46*–*49*). The diverse effects of the NF-κB pathway appear to be determined by the mechanisms sustaining tumor induction and by the type of immune response involved.

[1]Laboratory of Cancer Epigenetics, Faculty of Medicine, ULB (Université libre de Bruxelles)–Cancer Research Center (U-CRC), ULB, Brussels, Belgium. [2]Laboratory of Tumor and Development Biology, Groupe Interdisciplinaire de Génoprotéomique Appliquée (GIGA)–Cancer, University of Liège, Liège, Belgium. [3]Molecular Immunology Unit, Institut Jules Bordet, ULB, Brussels, Belgium. [4]Department of Cancer Biology, Vanderbilt-Ingram Cancer Center, Vanderbilt University, Nashville, TN 37232, USA. [5]Service of Molecular Virology, Department of Molecular Biology, U-CRC, ULB, Gosselies, Belgium. [6]Laboratory of Experimental Pathology, GIGA-Cancer, University of Liège, Liège, Belgium. [7]Breast Cancer Translational Research Laboratory, Jules Bordet Institute, ULB, Brussels, Belgium.
*These authors contributed equally to this work.
†Corresponding author. Email: agnes.noel@ulg.ac.be (A.N.); ffuks@ulb.ac.be (F.F.)

Growing evidence points to a link between cancer epigenetics and immunity. For instance, changes in 5mC have been found to correlate with the degree of immune infiltration of the tumor (*50*). Furthermore, epigenetic drugs have been shown to enhance the antitumor immune response (*51*–*53*). In addition, epigenetic enzymes, such as TETs, can regulate immune functions within leukocytes (*54*–*57*). The cross-talk between the immune system and cancer is thus of great importance, and investigating the underlying molecular mechanisms could lead to better therapeutic strategies.

The aim of the present work was to relate *TET* expression levels in BC to epigenetic anomalies and genes or pathways known to affect tumor growth and progression. We demonstrate for the first time that *TET1* repression and 5hmC changes are associated with activation of immune pathways and with tumor infiltration by immune cells. We further show, both in vitro and in mice, that activation of the major immune regulator NF-κB causes *TET1* repression by binding to its promoter. Our results also suggest that immunity-driven repression of *TET1* could occur in many cancer types. The exciting discovery that the immune system can influence the epigenetic state of cancer cells reveals a new dimension of the cross-talk between a tumor and its microenvironment.

RESULTS

TET1 regulation is associated with 5hmC changes in BLBC

To assess *TET1* expression in breast tumors, we used RNA sequencing (RNA-seq) data publicly available from "The Cancer Genome Atlas" (TCGA) consortium. Given the heterogeneity of mammary tumors, we divided samples into the four main BC subtypes and compared *TET1* expression in these subtypes and normal breast (Fig. 1A). As observed in previous studies (*18*, *22*), *TET1* expression was found to be decreased in luminal A ($n = 376$), luminal B ($n = 180$), and HER2-like ($n = 65$) tumors as compared to normal tissues ($n = 100$). BLBC tumors ($n = 130$) displayed a much wider range of *TET1* expression levels (approximately four times that of the other BC subtypes), with some tumors displaying abnormally high and others displaying abnormally low expression of the *TET1* gene.

We took advantage of the wide range of *TET1* expression in BLBC tumors to investigate the link between the 5hmC pattern and *TET1* regulation in these tumors. We performed mapping of 5hmC in matched tumor and normal breast tissues ($n = 4$ matched pairs), and we deposited raw data on the Gene Expression Omnibus (GEO) National Center for Biotechnology Information (NCBI) database (GSE101445). For this, we used a previously described approach (referred to here as "5hmC-seq"), combining the hMe-seal method (used to specifically select hydroxymethylated fragments) with deep sequencing (*58*). We then clustered breast sample pairs on the basis of *TET1* expression in the tumors. Characterization and segregation of the samples is shown in fig. S1. A comparison of *TET1*-low tumors with their matched normal tissues ($n = 2$ matched pairs) revealed 256 differentially hydroxymethylated regions (dhmRs), 58% of which were hypohydroxymethylated in the tumors. In the *TET1*-high tumors ($n = 2$ matched pairs), we identified 160 dhmRs, which were almost exclusively hyperhydroxymethylated (98%). All the identified dhmRs are displayed in a heat map in Fig. 1B, and the full list is detailed in table S1. The overlap of dhmRs between *TET1*-high and *TET1*-low groups was extremely low, with only two genes in common (*DNAH14* and *ABCA13*). These results indicate that BLBC tumors with different *TET1* expression levels display different 5hmC alteration patterns, high *TET1* expression

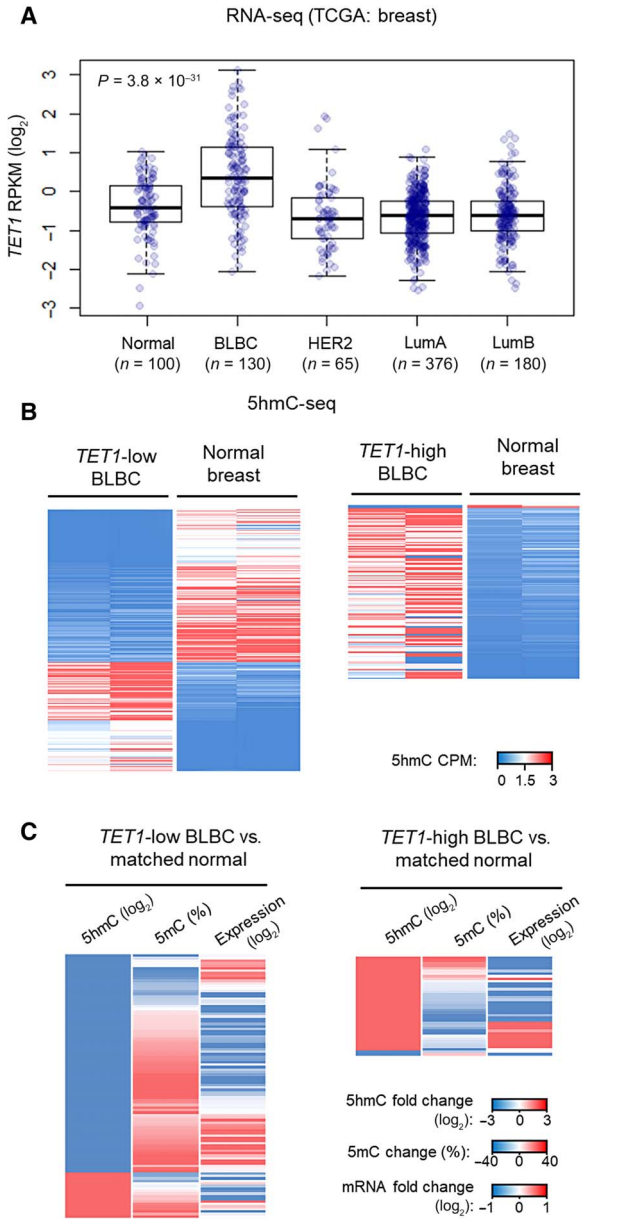

Fig. 1. *TET1* dysregulation is associated with an altered 5hmC pattern in BLBC. (**A**) *TET1* expression was assessed in RNA-seq data of the TCGA cohort ($n = 851$). Normal breast was compared to BC subtypes. Global comparisons between normal tissues and BC subtypes were performed by one-way analysis of variance (ANOVA). (**B**) Sequencing of 5hmC was performed in four pairs of matched BLBC and normal breast tissues. Paired samples were clustered on the basis of *TET1* expression in the tumor (high or low; see fig. S1). The heat maps illustrate the 256 and 160 dhmRs identified in BLBC tumors with low *TET1* expression (left; $n = 2$ matched pairs) and high *TET1* expression (right; $n = 2$ matched pairs), respectively. 5hmC levels are expressed in counts per million (CPM). (**C**) Heat maps illustrating 5hmC, 5mC, and gene expression changes in BLBC with low *TET1* expression (left) and high *TET1* expression (right), compared to normal breast tissue ($n = 2$ matched pairs per group). Only coding genes associated with dhmRs are represented for each tumor group. Changes in 5mC were measured with Illumina 450K Infinium in the same matched samples in which 5hmC was sequenced. The most variant probe of the corresponding region (promoter or gene body) is represented. Expression (mRNA) changes were obtained from TCGA by comparing reads per kilobase per million mapped reads (RPKM) values of the 25 BLBC tumors showing the lowest or highest *TET1* expression with those of normal breast tissue.

being mostly associated with 5hmC gain and low *TET1* expression being mostly associated with 5hmC loss.

In each BLBC group, we next investigated potential links between 5hmC, 5mC, and gene expression. DNA methylation was profiled in the same samples as 5hmC ($n = 2$ matched pairs per group), while expression changes were obtained from TCGA by comparing the 25 BLBC tumors showing the lowest or highest TET1 expression with those of normal breast tissue. We focused on all the coding genes associated with identified dhmRs (Fig. 1C). In the *TET1*-low group, 5hmC loss was mostly associated with 5mC gain. In the *TET1*-high group, consistently, 5hmC gain was mostly associated with 5mC loss. Precisely, changes in 5hmC and 5mC occurred in opposite directions in 73.7 and 70.2% of the dhmRs for the *TET1*-high and *TET1*-low groups, respectively, which was significantly more than expected by chance ($P = 0.003$ and $P < 0.0001$, respectively, by one-proportion z test). In both groups, the genes displaying 5hmC changes also showed dysregulated expression, although no association could be observed between the direction of these changes (by one-proportion z test). These data suggest that there is a link between DNA hydroxymethylation, DNA methylation, and gene expression in BLBC tumors. Together, these results indicate that, in BC, regulation of *TET1* expression (up or down) is associated with specific 5hmC changes, coupled with 5mC changes and altered gene expression.

In basal-like tumors, high *TET1* expression is associated with low levels of immune and defense response markers

To unravel the mechanisms responsible for *TET1* dysregulation in BC, we next investigated the relationship between *TET1* expression and signaling pathways. As BLBC tumors can display either high or low *TET1* expression, we focused on this subtype. From the TCGA RNA-seq data, we selected all the genes whose expression appeared to correlate positively (Pearson correlation coefficient $r > 0.25$) or negatively ($r < -0.25$) with *TET1* expression (in what follows, these genes will respectively be called "positively correlating" and "negatively correlating" genes). We then performed a gene ontology analysis with DAVID (tables S2 and S3). In the case of the negatively correlating genes, strikingly, the pathways most overrepresented were related to immunity and defense (Fig. 2A and table S2). To illustrate this result, we computed a heat map of the top 20 genes in the immune response category (Fig. 2B). The correlation coefficient calculated for these 20 genes combined was −0.49 ($P < 0.00001$) (Fig. 2B). In the other BC subtypes, the correlation between *TET1* expression and expression of the same 20 genes was much weaker (fig. S2), the combined r score being −0.18 ($P = 5 \times 10^{-4}$, $n = 376$) for luminal A tumors, −0.18 ($P = 0.016$, $n = 180$) for luminal B tumors, and −0.16 ($P = 0.18$, $n = 65$) for HER2-like tumors.

The abovementioned overrepresented pathways included both innate and adaptive immunity and the inflammatory response (Fig. 2A, and table S2). As shown in Fig. 2C and fig. S3A, we identified genes related to the myeloid/macrophage compartment, such as *TYROBP* and *CD14*, and to the lymphoid compartment, such as *CD3D*, *CD4*, *CD8A*, and *LST1*. The expression of genes encoding key regulatory factors involved in defense pathways, such as the NF-κB family member RELA, the major histocompatibility complex class I partner B2M, and the chemokine CCL2, was also found to correlate inversely with *TET1* expression (Fig. 2C, fig. S3A, and table S2).

Next, to quantify BLBC tumor infiltration by immune cells, we performed immunohistochemistry (IHC) targeting classical immune markers ($n = 18$). First, the percentage of $CD45^+$ cells, commonly used to score global leukocyte infiltration, was found to correlate negatively with *TET1* expression ($P = 0.02$; $n = 13$ versus $n = 5$ for *TET1*-low and *TET1*-high, respectively) (Fig. 3A). To score infiltration by T and B lymphocytes, we stained the CD3 and CD20 antigens, respectively, and again observed negative correlations with *TET1* expression ($P = 0.02$ and $P = 0.007$, respectively) (Fig. 3A). To further investigate the infiltrating cell populations in BLBC tumors, we then used CIBERSORT, a method for characterizing the cell composition of complex tissues on the basis of their gene expression profiles. Consistently with the IHC results (Fig. 3A), we found tumors with high *TET1* expression to display lower infiltration by $CD4^+$ and $CD8^+$ T lymphocytes ($P = 5 \times 10^{-5}$ and $P = 5 \times 10^{-6}$, respectively). They also showed lower infiltration by M1 and M2 macrophages ($P = 1 \times 10^{-4}$ and $P = 5 \times 10^{-4}$, respectively) (Fig. 3B and fig. S3B) and, importantly, a lower score for the NF-κB signature ($P = 4 \times 10^{-3}$; Fig. 3C).

Given the prognostic value of immune infiltration in BC, we next assessed the potential link between *TET1* expression and patient survival (fig. S3C). In public data sets, high *TET1* expression is associated with worse survival in BLBC, particularly as compared to *TET1*-low patients with high immune infiltration. This result contrasts with previously published results for *TET1* in BC (*18*) but agrees with the expected prognostic value of immune infiltration (*59*). Hence, the difference in survival might be driven by immune infiltration.

Last, we compared immune infiltration (assessed with CIBERSORT) in the four BC subtypes (fig. S4A). As described above, BLBC tumors with high *TET1* expression showed significantly lower mean levels of infiltration by most immune populations than their low *TET1* counterparts. In the other types, strikingly, no immune population (except B lymphocytes in luminal B) displayed any significant difference according to the level of *TET1* expression. This result suggests that the link between *TET1* and the immune infiltration is essentially specific to BLBC. The above findings thus indicate an association between the global immune state of BLBC and *TET1* expression and, more precisely, an anticorrelation between the level of *TET1* expression and the extent of infiltration by the major types of leukocytes.

TET1 expression is repressed by NF-κB activation

Since both the sizes of various immune cell populations and the levels of certain immune mediators (such as cytokines) were found to correlate negatively with *TET1* expression in BLBC, we hypothesized that leukocyte-driven activation of immune pathways might repress *TET1* expression in BC cells. This hypothesis is backed up by the observation that, in a public data set (GSE61208), *TET1* appears regulated upon immune modulation in breast tumors in mice (fig. S5A). To test this, we first treated MDA-MB-231 triple-negative BC cells with medium conditioned by myeloid U937 cells, and observed, by reverse transcription quantitative polymerase chain reaction (RT-qPCR), a significant decrease in transcript-level *TET1* expression (62% decrease; $P = 0.02$), but no change in *TET2* or *TET3* expression (Fig. 3D). Western blotting confirmed decreased TET1 production (Fig. 3D). Yet since U937 cells do not represent mature infiltrating macrophages, we further tested the effect of medium conditioned by polarized M1 and M2 macrophages (fig. S5C). M1-conditioned medium, but not M2-conditioned medium, caused *TET1* repression in MDA-MB-231 cells, suggesting that *TET1* might be regulated in BLBC by soluble factors secreted by specific immune subpopulations.

We next sought to unravel specific mechanisms of *TET1* regulation. As changes in *TET1* expression appeared to correlate with changes in tumor immune status, involving both innate and adaptive pathways and inflammatory markers as well (Fig. 2A), we hypothesized that a

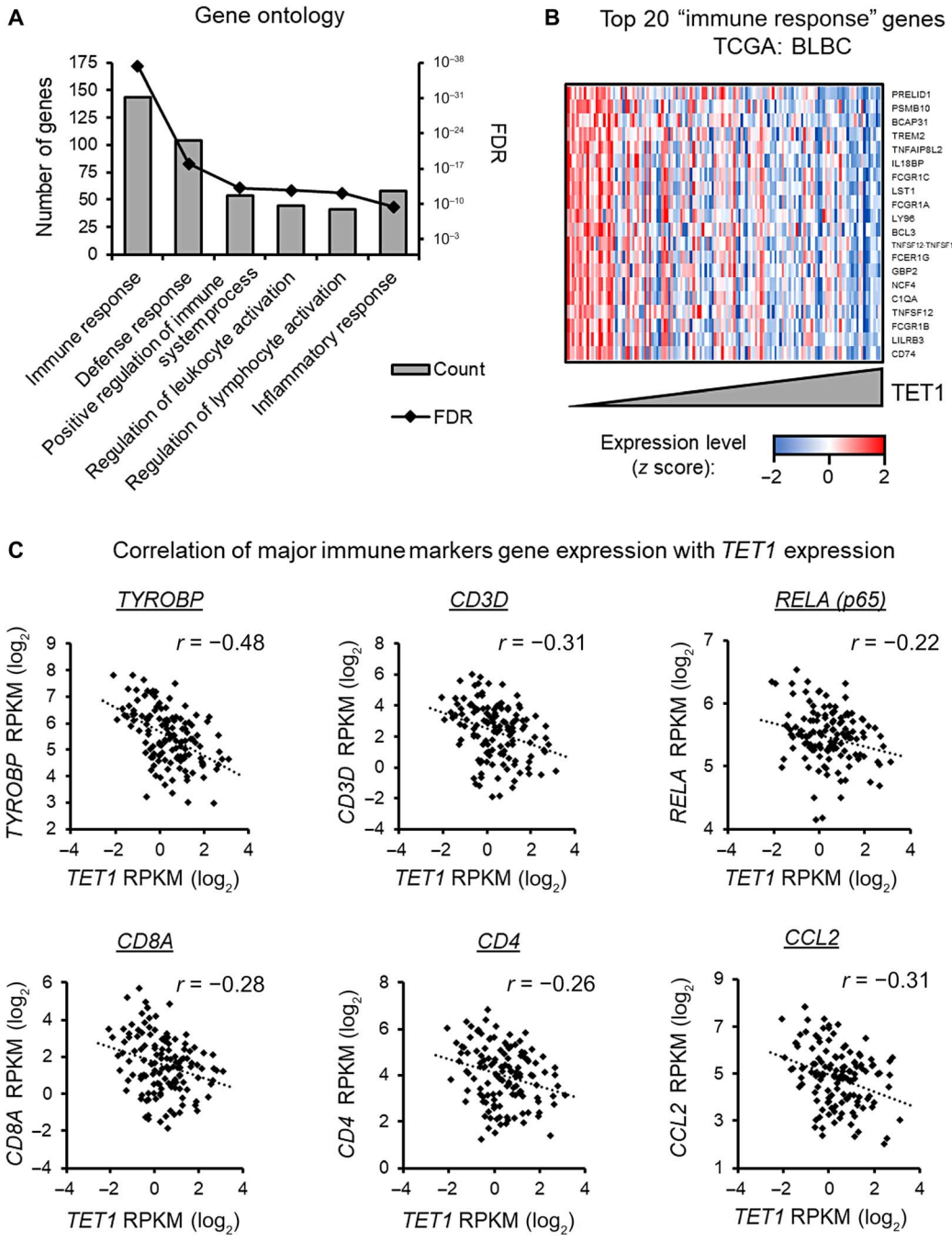

Fig. 2. High *TET1* expression defines a subgroup of BLBC with low levels of immune and inflammatory markers. (**A**) *TET1* expression correlates negatively with that of many genes linked to immunity, defense response, and inflammation pathways. Functional enrichment analysis was performed with DAVID on all genes whose expression showed a sufficient correlation ($r > 0.25$) or anticorrelation ($r < -0.25$) with *TET1* expression based on gene expression (RPKM) in TCGA BLBC samples ($n = 130$). The top 5 immune categories are represented. FDR, false discovery rate. (**B**) Heat map illustrating expression [RNA-seq by expectation maximization (RSEM) *z* score] of the top 20 genes in the "immune response" category of (A) based on the correlation coefficient *r*. TCGA BLBC samples were ordered by *TET1* expression level. (**C**) *TET1* anticorrelates with a broad range of immune markers, according to gene expression levels in TCGA BLBC samples. The genes concerned notably include those encoding monocyte marker *TYROBP*, lymphocyte markers *CD3D*, and the NF-κB family transcription factor *RELA* (p65). Additional examples are shown in fig. S3A.

central regulator might affect *TET1* expression. The NF-κB family transcription factors constitute a key regulatory family affecting many immune and inflammatory functions (*36*). The *RELA* gene, encoding the NF-κB family member p65, was among the genes whose expression was found to correlate negatively with *TET1* expression in BLBC tumors (Fig. 2C). Consistent with this, MDA-MB-231 cells treated with U937-conditioned medium displayed by Western blotting an increase in nuclear p65, indicative of activation of the canonical NF-κB pathway (Fig. 3D). In BLBC tissues, we also detected a link between high *TET1* expression and a low score for the NF-κB signature (Fig. 3C).

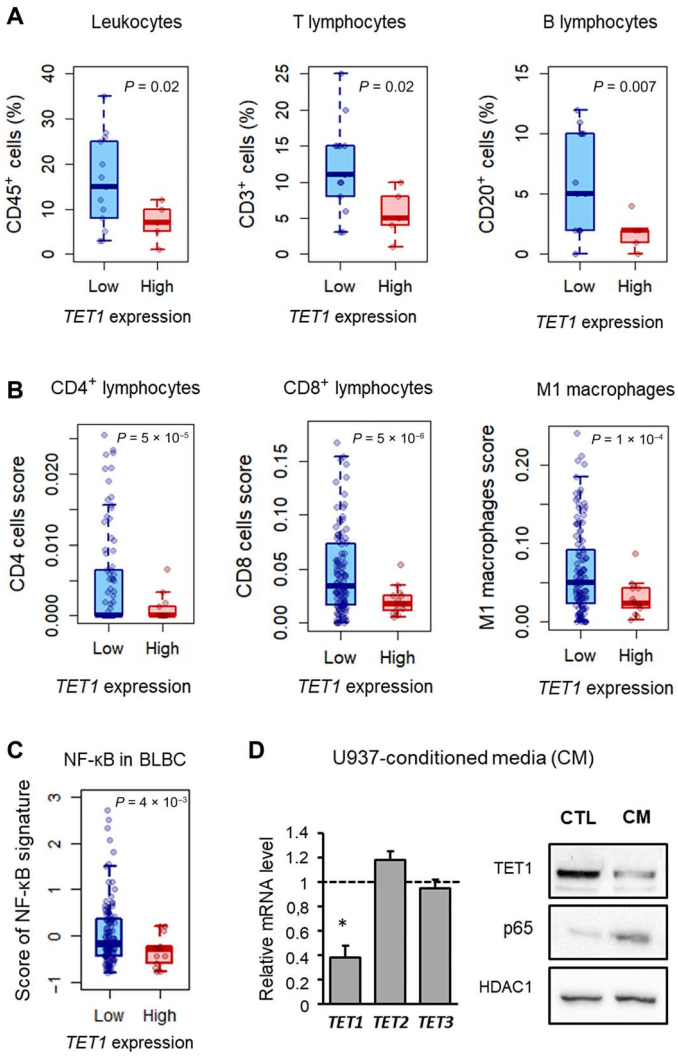

Fig. 3. High *TET1* expression distinguishes BLBC tumors with low immune infiltration and a low NF-κB signal. (**A**) High *TET1* expression is associated with low leukocyte infiltration in BLBC tumors. Tumor infiltration was measured by IHC. Staining for CD45, CD3, and CD20 was performed to quantify leukocytes, T lymphocytes, and B lymphocytes, respectively (n = 18). (**B**) Infiltration of BLBC tumors by major immune subpopulations was further analyzed by CIBERSORT, a method for characterizing the cell composition of complex tissues on the basis of their gene expression profiles (n = 130). Gene expression data (RPKM) were obtained from TCGA. (**C**) High *TET1* expression is associated with a weak NF-κB signature in BLBC tumors (n = 130). Gene expression data (RSEM z scores) were obtained from TCGA. (**D**) MDA-MB-231 cells were treated with medium preconditioned by U937 myeloid cells. Transcript-level *TET* expression was measured by RT-qPCR (left; n = 3; data expressed as means ± SD, relative to control) (*$P \leq 0.05$), and nuclear TET1 protein and p65 levels were assessed by Western blotting under control (CTL) conditions and in cells treated with conditioned medium (CM) (right).

In a publicly available data set (GSE52707), furthermore, p65 overexpression was found to cause reduced *TET1* expression (fig. S5B).

The above data suggest that NF-κB activation contributes to *TET1* repression. To test this hypothesis, different approaches were used to activate NF-κB. First, p65 was overexpressed in MDA-MB-231 cells, and reduced *TET1* expression was observed (41% decrease; P = 0.04) (Fig. 4A). This result is consistent with public data on p65 overexpression in BC cells (fig. S5B). Next, cells were treated with one of two well-established activators of the canonical NF-κB pathway (*60*), tumor necrosis factor (TNF) or lipopolysaccharide (LPS). This led, respectively, to a 45% (P = 0.01) or a 63% (P = 0.001) decrease in *TET1* production (Fig. 4, B and C, and fig. S6). When the same experiment was performed after pretreating the cells with MG-132, a known blocker of NF-κB activation (*61*), TNF-dependent repression of *TET1* was compromised (16% reduction; P = 0.15) (Fig. 4D). The effect of NF-κB activation on *TET1* expression was confirmed in two other triple-negative BC cell lines, Hs 578T and BT-549 (fig. S7, A and B). Of note, TNF and LPS specifically down-regulated *TET1* expression, with no effect on *TET2* expression and even a stimulation of *TET3* expression on occasion (Fig. 4, B and C).

To confirm *TET1* regulation in vivo, we used a transgenic mouse model (*IKMV* mice) in which aberrant NF-κB activation in the mammary epithelium leads to hyperplastic growth and ductal carcinoma in situ (*62*). Significantly reduced TET1 expression was detected in the carcinomas formed by both RT-qPCR (78% decrease; P = 0.001) and Western blotting (Fig. 4E).

In contrast to BLBC, other BC subtypes did not show reduced NF-κB signaling in *TET1*-high tumors (fig. S4B). In luminal (MCF7 and T47D) and HER2 (SKBR3) cell lines, no *TET1* repression was observed following TNF or LPS treatment (fig. S7, C to E). On the basis of control genes, the NF-κB response was also reduced as compared to triple-negative cells. This might explain, at least in part, the inability to regulate *TET1* in these cell lines.

In addition, and given the occasional changes of *TET2* and *TET3* expression upon immune modulation in vitro, we analyzed the potential association of these genes with immunity and NF-κB signaling in BLBC tissues (fig S8). *TET2* displayed a negative correlation with immune markers (r = −0.19, P = 0.03), but not to the extent of *TET1*. This association did not appear specifically linked to NF-κB (P = 0.26). Despite increased expression upon p65 overexpression and LPS treatment in vitro (Fig. 4, A and B), *TET3* also displayed a negative correlation with immune markers (r = −0.48, $P < 10^{-5}$), and NF-κB signaling was reduced in *TET3*-high tumors ($P = 1 \times 10^{-6}$). *TET3*- and *TET1*-high tumors thus displayed very similar patterns. In conclusion, there does not appear to be any compensation by either *TET2* or *TET3* in BLBC tumors.

Together, the above in vitro and in vivo results support the view that NF-κB activation negatively regulates *TET1* expression. This occurs specifically in BLBC.

TET1 is repressed through binding of NF-κB to its promoter

We next examined whether the NF-κB family transcription factor p65 might affect expression of *TET1* by binding to its promoter. In silico analyses performed with three different algorithms (JASPAR, AliBaba, and TFBIND) predicted two putative p65-binding sites (hereafter named sites A and B) in the *TET1* promoter, both located near the transcription start site (TSS) of the gene (Fig. 5A).

Luciferase assays were performed on extracts of MDA-MB-231 cells transfected with a TET1-LUC reporter. Upon NF-κB activation achieved by overexpressing p65 or by TNF treatment, the luciferase signal was found to decrease, indicating that the effect on *TET1* expression was, at least in part, promoter-dependent (Fig. 5B).

To assess binding of NF-κB to the *TET1* promoter in MDA-MB-231 cells, we conducted in vitro streptavidin-agarose pulldown assays. TNF treatment was found to induce binding of p65 to a *TET1* promoter probe containing the putative binding sites A and B (Fig. 5C). To confirm this result in an endogenous setting, we also performed chromatin immunoprecipitation (ChIP)–qPCR with a p65-targeting antibody. In TNF-treated cells, an average 2.7-fold enrichment was obtained with

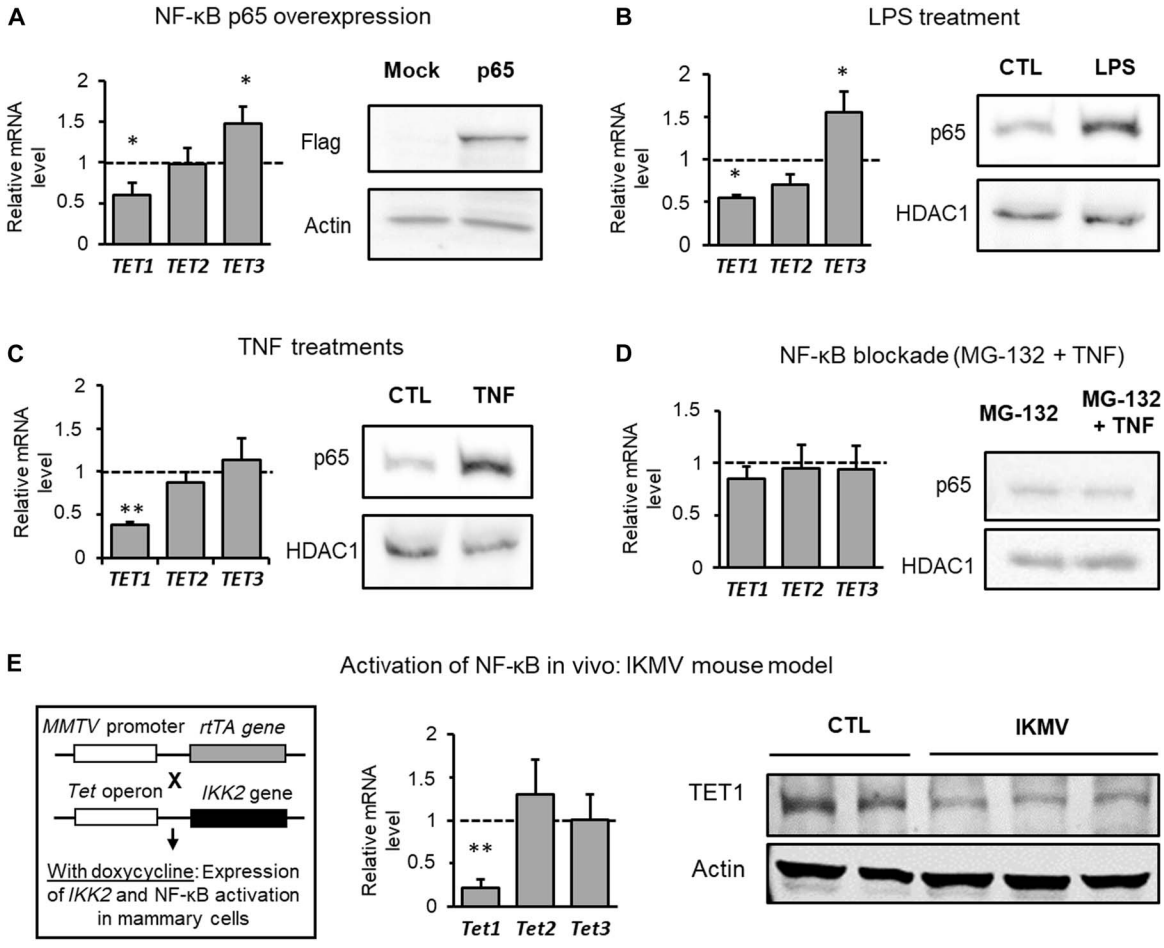

Fig. 4. *TET1* expression is repressed by NF-κB activation. (**A**) The gene encoding the NF-κB family member p65 was overexpressed in MDA-MB-231 cells (24 hours), and *TET* expression was measured by RT-qPCR (left; $n = 3$; data expressed as means ± SD, relative to control) (*$P \leq 0.05$). Nuclear p65 levels were assessed by Western blotting (right). (**B** and **C**) NF-κB was activated in MDA-MB-231 cells by treatment with LPS [(B) 5 mg/ml] or TNF [(C) 15 ng/ml] for 4 hours. *TET* expression was then measured by RT-qPCR (left; $n = 3$; data expressed as means ± SD, relative to control) (*$P \leq 0.05$; **$P \leq 0.01$). Nuclear p65 levels [LPS (5 mg/ml) or TNF (15 ng/ml); 30 min] were assessed by Western blotting (right). (**D**) TNF-dependent activation of NF-κB in MDA-MB-231 cells was blocked by pretreating the cells with MG-132 [20 μM; 3 hours before treatment with TNF (15 ng/ml) for 4 hours]. *TET* expression was measured by RT-qPCR (left; $n = 3$; data expressed as means ± SD, relative to control). Nuclear p65 levels [20 μM; 3 hours before treatment with TNF (15 ng/ml) for 30 min] were assessed by Western blotting (right). (**E**) The effect of NF-κB activation was assessed in vivo in the breast in the IKMV transgenic mouse model described by Barham *et al.* (*62*). *TET* expression was measured by RT-qPCR (left; $n = 3$; data expressed as mean ± SD, relative to control) (**$P \leq 0.01$), and the TET1 protein level was assessed by Western blotting (right; $n = 2$ controls versus 3 IKMV).

anti-p65, as compared to ChIP with a control immunoglobulin G (IgG) ($P = 0.03$) (Fig. 5D).

Given the close proximity of sites A and B (Fig. 5A), we used a streptavidin-agarose pulldown assay based on DNA probes to test them separately for p65 binding, as this allows better resolution than ChIP analysis. The assay was performed with a probe carrying either the wild-type version of the consensus NF-κB–binding sequence to be tested (A or B) or a disrupted version thereof (Fig. 5E and fig. S9). Strikingly, only the probe bearing the wild-type B site showed stronger p65 binding upon TNF treatment than its mutated counterpart. The above results suggest that *TET1* is repressed through binding of NF-κB to its promoter, the B site being the more potent binding site responsible for NF-κB–mediated regulation in BC cells.

TET1 is down-regulated by NF-κB in other cancer types

Given the broad involvement of NF-κB signaling in different cancer types, we screened the TCGA cohorts for other cancer types in which NF-κB–dependent regulation of *TET1* might occur. On the basis of RNA-seq data, several cancer types displayed a global immune status shift correlating with *TET1* expression, which was assessed with the 20-gene "immune signature" initially identified in BLBC (Fig. 2B). The list of TCGA cancer cohorts and their signature scores is provided in Table 1. Examples of cancers with a strong association between *TET1* and immunity include thyroid carcinoma (THCA), skin cutaneous melanoma (SKCM), and lung adenocarcinoma (LUAD). As shown in Fig. 6A, the immune signature correlated negatively with *TET1* expression in these three cancer types ($r = -0.39$, $P = 6 \times 10^{-20}$; $r = -0.36$, $P = 1 \times 10^{-15}$; and $r = -0.41$, $P = 9 \times 10^{-23}$) for THCA, SKCM, and LUAD, respectively. These cancers are all known to be infiltrated or surrounded by immunoreactive cells (*63*–*65*). Accordingly, the infiltration of most immune subpopulations, assessed with CIBERSORT, was found significantly decreased in tumors with high *TET1* expression (fig. S10A) in these cancer types, as observed in BLBC. However, other cancer types failed to display any significant correlation between

TET1 and the immune signature (Table 1). The spectrum of associations between *TET1* and tumor immunity is illustrated in fig. S11 for a representative panel of cancers, covering examples with strong [ovarian cancer (OV): $r = -0.58$, $P = 2 \times 10^{-29}$], intermediate [prostate adenocarcinoma (PRAD): $r = -0.24$, $P = 1 \times 10^{-7}$], and nonsignificant [kidney renal clear cell cancer (KIRC): $r = -0.02$, $P = 0.62$; and colon adenocarcinoma (COAD): $r = 0.03$, $P = 0.68$] correlations. As expected, the association between *TET1* and immune markers or tumor immune infiltration was strongest in OV and markedly reduced in PRAD, KIRC, and COAD.

Next, we investigated the potential link between NF-κB signaling and *TET1* regulation. Consistent with the results obtained for BLBC, high expression of *TET1* was associated with a weak NF-κB signature in THCA, SKCM, and LUAD (Fig. 6B). We tested the effect of NF-κB activation by TNF in vitro in cell lines derived from THCA, SKCM, and LUAD tumors (respectively the TPC1, A375, and A579 cell lines) (Fig. 6C and fig. S10B). Decreased *TET1* expression was consistently observed in all three cell lines (respectively a 69% decrease with $P = 0.0001$, a 47% decrease with $P = 0.02$, and a 38% decrease with $P = 0.03$). High expression of *TET1* was also associated with reduced NF-κB signaling in OV (fig. S12A), and in vivo inhibition of NF-κB in ID8 mouse OV cells induced *TET1* expression (fig. S12B). NF-κB–dependent regulation of *TET1* is thus not only restricted to BLBC but can also occur in other tumors. In contrast, the association between *TET1* and NF-κB signaling was either reduced or absent in PRAD, KIRC, and COAD (fig. S12, A and C to E).

Last, streptavidin-agarose pulldown assays performed with the probe bearing the wild-type NF-κB binding site B confirmed that p65 can bind to the *TET1* promoter upon TNF induction in TPC1, A375, and A549 cells (Fig. 6D and fig. S10C). Disruption of the B-site NF-κB consensus sequence was found to decrease this binding. Only in A549 cells, however, did the A site show reduced binding upon disruption of the NF-κB consensus sequence (fig. S10D). This suggests that, while p65 can also bind to the A site, the B site is favored in most cellular contexts. Together, these results suggest that the mechanism by which immunity drives *TET1* down-regulation through NF-κB activation and binding to the *TET1* promoter is not restricted to BLBC and may instead be common to many cancer types, such as melanoma and thyroid, lung, and ovarian cancers.

DISCUSSION

Dysregulation of TETs and 5hmC has been described as a hallmark of cancer, with implications for progression of the disease (*17*, *66*, *67*). In BC, *TET1* down-regulation has been suggested to enhance tumor progression and metastasis (*18*, *24*). Here, our investigation of the regulation of TETs and 5hmC in cancer has led us to address the essential question of the cross-talk between cancer cells and their immune microenvironment and to uncover a mechanism through which the immune system can regulate the epigenetic state of cancer cells, and hence their gene expression pattern, via TETs.

As *TET* down-regulation is observed in nearly all cancer types, our starting hypothesis was that alterations in signaling pathways frequently associated with tumors could play a role in this regulation. Our gene ontology analysis, applied to the genes whose expression anticorrelates with *TET1* expression in the BLBC subtype, predominantly highlighted immune pathways. Accordingly, tumors where *TET1* was repressed were found to show high expression of immune genes and high infiltration by major immune populations, including B lymphocytes, $CD4^+$ and

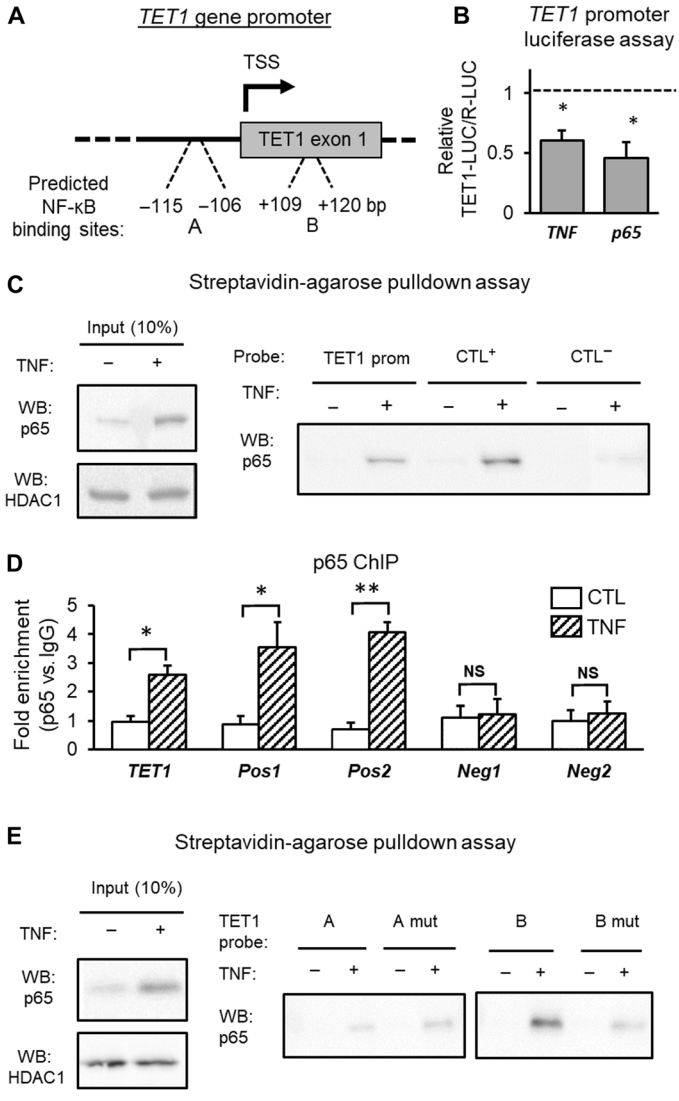

Fig. 5. NF-κB represses *TET1* gene expression by binding to its promoter. (**A**) Schematic view of the *TET1* gene promoter. Two NF-κB binding sites, named "A" and "B," were identified. Binding site locations are indicated relative to the *TET1* TSS. (**B**) *TET1* promoter activity was assessed under NF-κB activation by cotransfecting MDA-MB-231 cells with a vector encoding firefly luciferase under the control of the *TET1* promoter (TET1-LUC) and a control vector encoding Renilla luciferase (R-LUC) before treating the cells with TNF (15 ng/ml, 24 hours) or overexpressing p65 (24 hours) ($n = 3$, data expressed as means ± SD). Results are expressed relatively to control conditions (*$P \leq 0.05$). (**C**) Streptavidin-agarose pulldown assays were performed to assess binding of p65 to the *TET1* promoter in vitro. Pulldown of nuclear proteins extracted from MDA-MB-231 cells was achieved with biotinylated DNA probes corresponding to the *TET1* promoter (TET1 prom) and with positive/negative control probes (CTL^+/CTL^-). TNF treatment (15 ng/ml, 30 min) was used to induce nuclear translocation of p65. (**D**) ChIP was performed with a p65-targeting antibody or a control IgG to assess p65 binding to the *TET1* promoter in MDA-MB-231 cells. TNF treatment (15 ng/ml, 30 min) was used to induce nuclear translocation of p65. NS, not significant (*$P \leq 0.05$; **$P \leq 0.01$). (**E**) Streptavidin-agarose pulldown assays were performed with biotinylated DNA probes corresponding to the predicted NF-κB binding site A or B. To assess the binding specificity, pulldowns were done with either the wild-type site or a mutated version in which the consensus NF-κB–binding sequence was disrupted (wild-type probes: A and B; mutated probes: A mut and B mut). TNF treatment (15 ng/ml, 30 min) was used to induce nuclear translocation of p65.

Table 1. *TET1* expression correlates negatively with immune markers in many cancer types. The correlation between *TET1* expression and the score of the "top 20 immune signature" (defined in Fig. 2) were computed for all TCGA cancer cohorts. The name of the disease and the TCGA acronym, the Pearson correlation coefficient, the associated *P* value, and the number of cancer samples are indicated for each cohort.

Cancer type	TCGA cohort	Pearson	*P*	Number of samples
Ovarian serous cystadenocarcinoma	OV	−0.58	2.1×10^{-29}	307
Glioblastoma multiforme	GBM	−0.56	7.4×10^{-15}	166
Sarcoma	SARC	−0.50	9.6×10^{-18}	263
Brain lower grade glioma	LGG	−0.46	1.0×10^{-28}	530
Uterine carcinosarcoma	UCS	−0.44	5.7×10^{-4}	57
Lung adenocarcinoma	LUAD	−0.41	9.0×10^{-23}	517
Mesothelioma	MESO	−0.41	6.9×10^{-5}	87
Thyroid carcinoma	THCA	−0.39	5.6×10^{-20}	509
Cholangiocarcinoma	CHOL	−0.38	2.1×10^{-2}	36
Uterine corpus endometrial carcinoma	UCEC	−0.36	9.1×10^{-7}	177
Skin cutaneous melanoma	SKCM	−0.36	1.1×10^{-15}	472
Kidney renal papillary cell carcinoma	KIRP	−0.33	4.9×10^{-9}	291
Uveal melanoma	UVM	−0.32	4.0×10^{-3}	80
Lung squamous cell carcinoma	LUSC	−0.32	4.3×10^{-13}	501
Pheochromocytoma and paraganglioma	PCPG	−0.31	2.2×10^{-5}	184
Testicular germ cell tumors	TGCT	−0.28	4.0×10^{-4}	156
Thymoma	THYM	−0.28	2.1×10^{-3}	120
Adrenocortical carcinoma	ACC	−0.25	2.9×10^{-2}	79
Prostate adenocarcinoma	PRAD	−0.24	9.6×10^{-8}	498
Head and neck squamous cell carcinoma	HNSC	−0.18	3.0×10^{-5}	522
Kidney chromophobe	KICH	−0.17	1.8×10^{-1}	66
Cervical and endocervical cancers	CESC	−0.13	2.0×10^{-2}	306
Bladder urothelial carcinoma	BLCA	−0.09	7.6×10^{-2}	408
Stomach adenocarcinoma	STAD	−0.06	2.1×10^{-1}	415
Kidney renal clear cell carcinoma	KIRC	−0.02	6.2×10^{-1}	534
Liver hepatocellular carcinoma	LIHC	0.02	6.8×10^{-1}	373
Colon adenocarcinoma	COAD	0.03	6.8×10^{-1}	191
Esophageal carcinoma	ESCA	0.04	6.2×10^{-1}	185
Rectum adenocarcinoma	READ	0.04	7.1×10^{-1}	72
Pancreatic adenocarcinoma	PAAD	0.19	9.7×10^{-3}	179

$CD8^+$ T lymphocytes, and macrophages. We provide evidence that soluble factors secreted by immune cells, such as M1 macrophages, could be responsible for *TET1* modulation in BLBC. One factor abundantly secreted by M1 (but not M2) macrophages is TNF (*68*, *69*), which is sufficient to cause *TET1* repression. Thus, secretion of TNF by infiltrating macrophages might be involved in *TET1* repression. This is most interesting, as interactions between tumors and the immune system have emerged in recent years as important in cancer (*25*). Infiltration of the tumor by immune cells is observed in many types of cancer. It is, at least in part, due to secretion of recruiting factors by cancer cells themselves and has major impacts in terms of disease progression and response to treatment (*36*).

The immune system has a dual action in cancer (*25*). On the one hand, secretion of proinflammatory factors appears to enhance

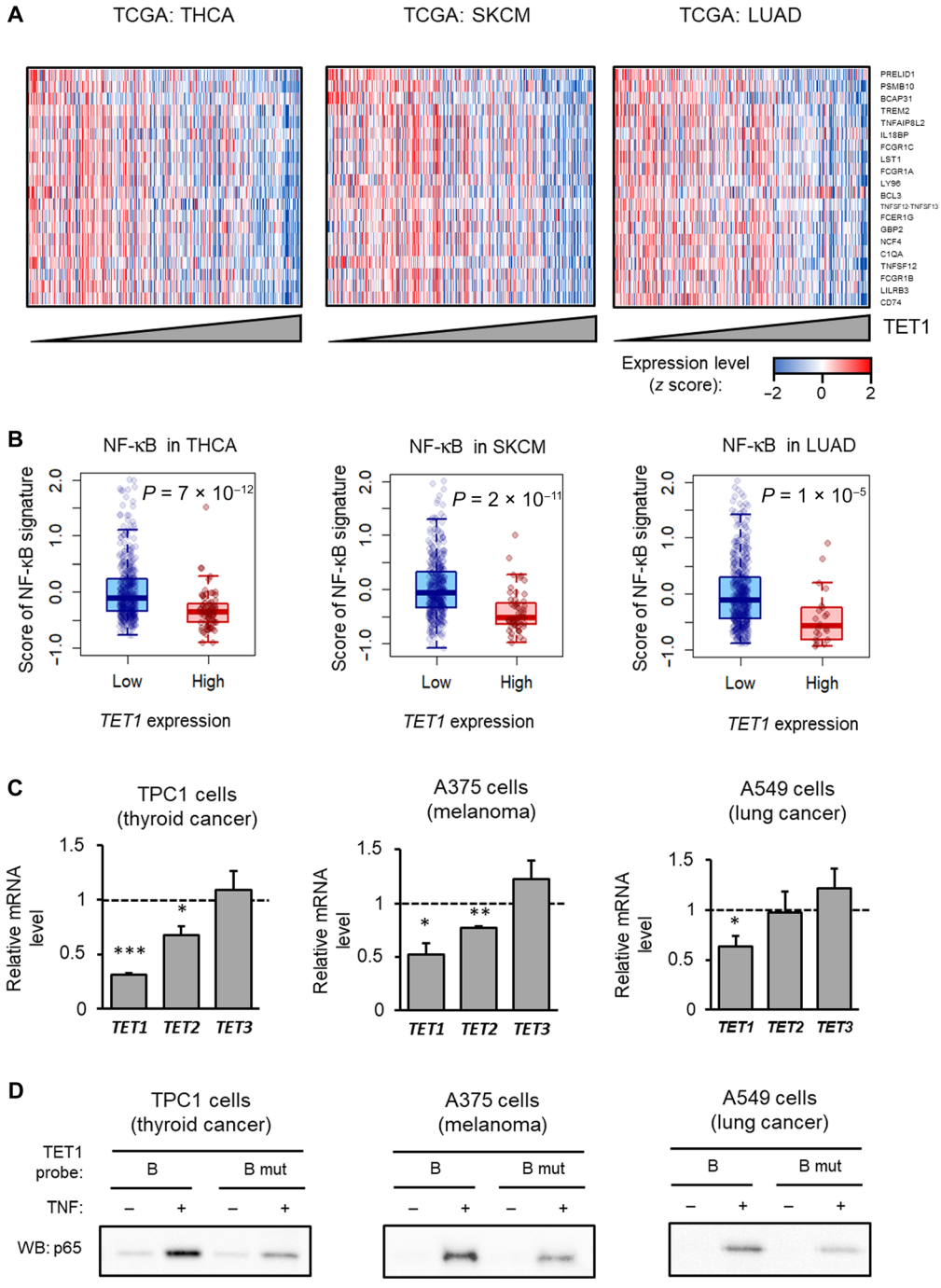

Fig. 6. *TET1* and NF-κB in other cancer types. (**A**) Heat map illustrating expression (RSEM *z* score) of the "20–immune response gene" signature of Fig. 2B in several cancer types (from left to right: THCA SKCM, and LUAD). Data were taken from the TCGA cohort and ordered by *TET1* expression in each cancer type. (**B**) High expression of *TET1* is associated with a weak NF-κB signature in THCA ($n = 509$), SKCM ($n = 472$), and LUAD ($n = 510$) tumors. Gene expression data (RSEM *z* scores) were obtained from TCGA. (**C**) NF-κB was activated by treating TPC1 thyroid cancer cells, A375 melanoma cells, and A549 lung cancer cells with TNF for 4 hours. *TET* expression was measured by RT-qPCR ($n = 3$; data expressed as means ± SD, relative to control) (*$P \leq 0.05$, **$P \leq 0.01$, and ***$P \leq 0.001$). (**D**) Streptavidin-agarose pulldown assays were performed as described above to assess in vitro the binding of NF-κB family member p65 to the *TET1* promoter in TPC1, A375, and A549 cells [TNF (15 ng/ml), 30 min].

cancer progression and favor resistance to treatment. On the other hand, antitumor immune responses, and particularly TILs, are increasingly recognized as associated with better clinical outcome in many cancers (*26*–*28*). The prognostic value of *TET1* expression in cancer might be related to the immune status of the tumor. Also central is the recent emergence of novel and promising immunotherapeutic tools (for example, PD-L1 and PD-1 inhibitors) used to prevent cancer from escaping destruction by the immune system. These tools have raised new hopes for better cancer treatment (*29*).

We have specifically linked *TET1* repression to NF-κB. This major immunoregulatory transcription factor is known to be activated in many cancer types (*36*). It is mostly viewed as protumorigenic, particularly when its activation is associated with an inflammatory context, but NF-κB signaling can also be a marker of an immune response targeting malignant cells (*35*, *70*). Here, we have found the NF-κB family member p65 to be involved in *TET1* repression. Generally speaking, the p65-p50 heterodimer is recognized as promoting the expression of many cytokines and chemokines, while repressive activity is more often attributed to the p50-p50 homodimer. Yet there are also reports of a repressive effect of p65-p50, exerted through interaction with co-repressors such as histone deacetylases (HDACs) or DNA methyltransferases (*33*, *71*). Our study thus highlights the dual function (both activating and repressing) of this transcription factor in gene regulation while revealing a new facet of its role in cancer signaling: an involvement in epigenetic regulation.

We have extended to other cancers our findings concerning BLBC. We have notably demonstrated in THCA, SKCM, LUAD, and OV an anticorrelation between *TET1* expression and the 20-gene immune signature described for BLBC. We have also shown in cell lines derived from these tumor types that NF-κB represses *TET1* by binding to its promoter. We have thus uncovered what appears as a commonly occurring novel link between *TET1* regulation and the immune system in cancer.

The finding that epigenetics and immunity are interwoven in cancer has been increasingly highlighted. Altered DNA methylation, particularly, has been linked to the presence of infiltrating immune cells (*50*). The present study highlights a new dimension of the epigenetics-immunity connection: immunity-driven repression of *TET1* in cancer cells. Thus far, TET enzymes have been implicated only in the regulation of immune cells themselves. In regulatory T cells, for instance, TETs promote *FOXP3* expression and T_{reg} cell–associated immune homeostasis (*72*). In myeloid cells, TET2 controls inflammation by repressing the proinflammatory cytokine *IL6* (*54*). TET2 has also been found to promote activation of cytokine genes in $CD4^+$ T cells (*55*). Furthermore, TET1 has been reported as an epigenetic regulator involved in T helper 2 cell differentiation (*57*). Here, for the first time, we show that the link between immune pathways and TETs extends beyond the immune system itself. Specifically, we provide evidence that NF-κB–mediated regulation of *TET1* occurs in both BC and other cancer cells.

In conclusion, our data reveal a novel function of NF-κB, a factor known to orchestrate immune and inflammatory responses and oncogenesis (*63*–*65*, *70*). Although identified in BLBC, NF-κB–mediated repression of *TET1* appears to be common to many cancer types. Given the link between *TET1* repression and immunity and the importance of immune infiltration in predicting clinical outcome, it is worth rethinking how *TET1* expression relates to cancer. This is of great importance, as epigenetic drugs have been shown to modulate the antitumor immune response, and dissecting the epigenetic mechanisms underlying the cross-talk between the immune system and cancer could help optimize therapeutic strategies.

MATERIALS AND METHODS

Human cancer data sets

TCGA gene expression data sets (RNA-seq sequencing RPKM and RSEM) were downloaded from the "firehose" website (https://gdac.broadinstitute.org/). For correlation analysis, a $\log_2$ transformation was applied to the expression values, and then the Pearson scores for the correlation of all genes with *TET1* expression were computed. Functional enrichment analysis was performed with DAVID (version 6.7) (*73*). For all TCGA analyses, the top 10% of each cohort was considered "*TET1*-high," the rest being considered "*TET1*-low." The same cutoff was applied for *TET2* and *TET3* in TCGA analyses. For the other cohorts, given the smaller number of samples available, all percentiles were computed, and the best-performing threshold (in terms of the *P* value for the corresponding observation, regardless of the direction of the change) between the two groups was selected as the cutoff.

Immune infiltration in TCGA cohorts was quantified on the basis of expression data with the CIBERSORT algorithm (https://cibersort.stanford.edu/). Briefly, this algorithm can accurately estimate levels of many different leukocyte subsets in bulk tumor samples profiled by array or RNA-seq on the basis of a signature of 547 distinct genes distinguishing leukocyte subpopulations (*74*). The signature was built from public expression data sets of leukocyte subpopulations and was optimized to include the most relevant differentially expressed genes. Then, a deconvolution method was applied to separately quantify each population. The NF-κB signature score was based on the mean expression (RNA-seq RPKM) of eight target genes, as previously reported (*75*).

Cell culture and treatments

MDA-MB-231 and A549 cells were purchased from Caliper Life Sciences. Hs 578T, BT-549, MCF-7, T47D, SKBR3, 786-O, HT29, PC3, THP-1, and U937 cells were obtained from the American Type Culture Collection. A375 and TPC1 cells were provided, respectively, by J.-C. Marine (Katholieke Universiteit Leuven, Belgium) and C. Maenhaut [Université libre de Bruxelles (ULB), Belgium]. All cells were grown at 37°C under 5% CO_2. MDA-MB-231, A549, Hs578T, A375, BT-549, MCF-7, T47D, SKBR3, and TPC1 cells were cultured in Dulbecco's modified Eagle's medium (Gibco) supplemented with 10% fetal bovine serum (FBS) (Gibco), 1% L-glutamine (Gibco), and 1% penicillin and streptomycin (Gibco). PC3 cells were cultured in Ham's F-12K (Kaighn's) Medium (Gibco) supplemented with 10% FBS (Gibco) and 1% penicillin and streptomycin (Gibco). U937, HT29, THP-1, and 786-O cells were cultured in RPMI 1640 (Invitrogen) supplemented with 10% FBS.

To produce U937-conditioned medium, U937 cells (seeded at 1×10^6 cells/ml) were grown for 48 hours, washed with phosphate-buffered saline (PBS), and incubated for another 24 hours in a serum-free medium. The supernatant was collected and centrifuged in Christ RVC 2-18 CDplus (Martin Christ) according to Mohamed (*76*). MDA-MB-231 cells were split at low density (40% of confluence) and maintained in culture for 48 hours before treatment with U937-conditioned medium, human recombinant TNF (15 ng/ml) (PHC3015, Gibco), or LPS (5 μg/ml) (L2630, Sigma-Aldrich). To obtain M1 macrophage– and M2 macrophage–conditioned medium, THP-1 monocytes (seeded at 7×10^5 cells/2 ml) were first differentiated to macrophages in the course of a 24-hour incubation with phorbol 12-myristate 13-acetate (20 ng/ml) (PMA; P8139, Sigma) in RPMI 1640. Then, the macrophages were polarized either to M1 macrophages by 48 hours of incubation with interferon-γ (20 ng/ml) (300-02, Peprotech) and LPS (50 ng/ml) (L6529, Sigma) or to M2 macrophages by 48 hours of incubation with interleukin-4 (IL-4) (20 ng/ml) (11340045, ImmunoTools). The supernatants were collected and centrifuged at 200*g* for 5 min at 4°C. Cancer cells were split at low density (40% confluence) and

maintained in culture for 24 hours before treatment with U937-, M1 macrophage–, or M2 macrophage–conditioned medium, human recombinant TNF (15 ng/ml) (PHC3015, Gibco), or LPS (5 μg/ml) (L2630, Sigma-Aldrich). Cells were collected at different times according to the analysis (30 min, 4 hours, or 24 hours). To inhibit the NF-κB pathway, cells were pretreated with 20 μM MG-132 (M7449, Sigma-Aldrich) for 3 hours before TNF treatment. In some assays, cells transfected with p65 complementary DNA (cDNA) were used. Transfection was performed with Lipofectamine 2000 reagent according to the manufacturer's instructions, and cells were collected after 24 hours.

Mouse experiments

RNA and nuclear proteins were extracted from mammary glands of the transgenic IKMV mice, a doxycycline-inducible transgenic mouse model in which active IKK2 is expressed in the mammary epithelium. The mice were provided by F. Yull of the Vanderbilt-Ingram Cancer Center, Nashville and are described in the study of Barham *et al.* (*62*). Three wild-type and three IKMV mice treated with doxycycline for 3 days were used for analyses.

C57BL/6 mice injected intraperitoneally with ID8 mouse ovarian cancer cells were treated thrice weekly intraperitoneally for 10 days with vehicle (1% dimethyl sulfoxide in PBS) or the NF-κB inhibitor thymoquinone (TQ; 40 mg/kg). Expression of *TET1* was measured in 20 μg of whole-cell protein extracts from harvested peritoneal tumors by Western blot. Three control mice and three TQ-treated mice were used for analyses. The experimental protocols were reviewed and approved by the Institutional Animal Care and Use Committee at Vanderbilt University.

Reverse transcription quantitative polymerase chain reaction

Total RNA was extracted with the High Pure RNA Isolation Kit (Roche) or the RNeasy Mini Kit (Qiagen). RNA was quantified with an ND-100 NanoDrop Spectrophotometer. One microgram of total RNA was reverse-transcribed with the First Strand cDNA Synthesis Kit (Roche) according to the manufacturer's recommendations. Real-time PCR was performed with the LightCycler 480 Probes Master Kit (Roche) and the Universal ProbeLibrary System (Roche) or Brilliant SYBR Green QPCR Master Mix (Roche). Gene expression was normalized to human glyceraldehyde phosphate dehydrogenase and hypoxanthine phosphoribosyltransferase 1 (HPRT1) or to mouse actin and 18*S*. Primer sequences are indicated in table S4.

Western blotting and streptavidin-agarose pulldown assays

Nuclear and cytosolic extracts were prepared according to methods described previously (*77*). Fifty micrograms of extract was electrophoresed through an 8% SDS–polyacrylamide gel, transferred onto a polyvinylidene difluoride membrane (PerkinElmer) at 110 V for 80 min, and subjected to Western blot analysis. Antibodies against TET1 (1:500; 09-872, EMD Millipore), p65 (1:500; ab7970, Abcam), HDAC1 (1:1000; C15410053, Diagenode), actin (1:2000; A5316, Sigma), or Flag (1:1000; F3165, Sigma-Aldrich) were used and diluted in 5% (w/v) nonfat dry milk in PBS containing 0.1% Tween 20. Secondary antibodies were GE Healthcare NA934V (1:5000) for anti-rabbit antibodies and NXA931 (1:3000) for anti-mouse antibodies. Actin and HDAC1 were used as loading controls. Western blots were visualized with the ECL Plus system (Amersham Biosciences).

Streptavidin-agarose pulldowns were performed to evaluate protein binding to DNA. The protocol was adapted from Deng *et al.* (*78*). Briefly, 500 μg of nuclear proteins and 5 μM biotinylated DNA probe were incubated overnight at 4°C under rotation in buffer A [10 mM Hepes (pH 7.9), 10 mM KCl, 0.1 mM EDTA, 1 mM dithiothreitol, 0.4% NP-40, and antiproteases (11836153001, Roche)]. The extracts were then incubated for 1 hour at room temperature with 50 μl of streptavidin beads (20357, Thermo Fisher Scientific). After four washes with 400 μl of buffer A, the beads were heated for 5 min at 95°C in 20 μl of Laemmli buffer and analyzed by Western blotting.

Immunohistochemical staining

Quantification of immune cells by pathologists was performed as previously described (*79*). Staining of formalin-fixed paraffin-embedded tissue sections (4 μm thick) was performed with a BenchMark XT IHC/ISH automated slide stainer (Ventana Medical Systems Inc.). The antibodies used for immunohistochemical staining were anti-CD45 (Dako Denmark A/S), anti-CD3 (Dako Denmark A/S), and anti-CD20 (Dako Denmark A/S). They were revealed with the ultraView Universal DAB Detection Kit (Ventana Medical Systems Inc.). All staining reagents used were manufactured by Roche (F. Hoffmann–La Roche Ltd.). Images were analyzed with VisiomorphDP software (Visiopharm) to quantify the $CD45^+$, $CD3^+$, and $CD20^+$ areas within the invasive tumor area defined for each digital image. The total positively stained area was scored as a percentage of the defined region, and the mean percentage of the scores obtained by two or three different pathologists was calculated for each sample. *TET1* expression data for the IHC samples were taken from the Affymetrix data set GSE20711. The BLBC samples from this cohort were then separated into two groups (TET1-low and TET1-high), the cutoff being chosen to optimize the significance for $CD45^+$ quantification between the two groups. The same split was then used for $CD3^+$ and $CD20^+$ quantification.

Survival analyses

Kaplan-Meier survival curves and log-rank tests were used to assess the prognostic value of *TET1* expression in BLBC. Several sets from the GEO data repository were combined (regardless of treatment), and the entire collection of probe sets of the Affymetrix Human Genome U133 Plus 2.0 Array was reannotated, as previously described (*80*). Groups were distinguished on the basis of *TET1* expression alone (left panel), or in combination with the TIL score (middle panel), and relapse-free survival was analyzed. For overall survival analysis, data were obtained from GSE16446. In this cohort, all patients were specifically treated with anthracycline (epirubicin) neoadjuvant therapy. *TET1* expression was obtained for each sample from the microarray data of the corresponding cohort. Then, all percentiles were computed, and the best-performing threshold between the two groups (*TET1*-high and *TET1*-low) was selected as the cutoff.

Chromatin immunoprecipitation

MDA-MB-231 cells were treated with TNF (30 min), and then chromatin was extracted with the ChIP-IT High Sensitivity Kit (Active Motif). Briefly, the cells were cross-linked for 10 min with Complete Cell Fixation Solution (1:10 growth medium volume). The reaction was stopped with 1/20 volume of Stop Solution. Extracts were washed twice with cold PBS. Sonication was performed with Bioruptor Plus. The following settings were used to get chromatin fragments 200 to 500 base pairs (bp) long: 35 min of sonication, strength set at high, with 30-s on/off intervals. Sheared chromatin (30 μg) was incubated overnight at 4°C with 4 μg of rabbit polyclonal antibody against p65 (SC-372, Santa Cruz Biotechnology) or control IgG (SC-2027, Santa

Cruz Biotechnology). Antibody-bound protein/DNA complexes were then immunoprecipitated with Protein G agarose beads. Finally, the eluted chromatin was subjected to reverse cross-linking, digestion with proteinase K, and DNA purification, according to the instructions of the IT High Sensitivity Kit. Enrichment in the p65 immunoprecipitate was measured by qPCR. Positive control sequences 1 and 2 (NF-κB response genes PTGES2 and IL-10) and negative control sequences 1 and 2 (intergenic regions of chromosomes 14 and 10) were chosen on the basis of public p65 ChIP-seq data (GSM1055811).

Luciferase assay

Luciferase assays were performed with the Dual-Glo Luciferase Assay System (E2920, Promega). Briefly, cells at 70 to 80% confluence were cotransfected with the TET1-LUC and Renilla-LUC vectors at ratio 1:5. Twenty-four hours after transfection, the cells were lysed, and the firefly signal was measured using a luminometer (Promega Turner Designs Luminometer TD-20/20). TET1-LUC reporter activity was then normalized to Renilla-LUC activity.

5hmC-seq and bioinformatics analyses

TET1 expression was measured by RT-qPCR in four pairs of matched tumor (BLBC) and normal breast tissues. Tumors (and their corresponding normal tissues) were divided into *TET1*-high (n = 2 pairs) and *TET1*-low (n = 2 pairs) on the basis of *TET1* expression.

The genome-wide distribution of 5hmC was determined by hydroxymethylated DNA fragment affinity purification (hMe-seal), as previously described (*58*). DNA was fragmented using a Bioruptor sonicator (Diagenode) to obtain fragments averaging 300 bp in size, and enrichment in hydroxymethylated fragments was performed from 500 ng of DNA with the hydroxymethyl collector (Active Motif) according to the manufacturer's protocol. Library preparation was done with the TruSeq ChIP Sample Prep Kit (Illumina) according to the manufacturer's instructions.

The Bowtie2 software was used to map sequencing reads to the human genome [NCBI Build 37/University of California, Santa Cruz (UCSC) hg19]. Raw data are available in the GEO database (GSE101445). After removing duplicate reads (that is, reads mapping to the same location) with Picard Tools software, read density was computed by counting the reads in nonoverlapping 2-kb windows tiling the whole genome, thanks to the featureCounts software. Reads mapping to multiple locations in the reference genome or overlapping two windows were fractionated among the associated windows. Windows presenting a significantly different 5hmC level between tumor samples and adjacent normal tissues were identified with edgeR software ($\log_2$ fold change > 3 and false discovery rate < 0.05). As for each patient, a tumor sample and an adjacent normal tissue were available, and paired analysis was applied.

For annotation purposes, enhancers were obtained from the EnhancerAtlas prediction database (www.enhanceratlas.org/; downloaded in June 2016), gene bodies were defined as regions from TSS to transcription termination site of RefSeq genes (downloaded from UCSC on 25 November 2015), and promoters were defined as ranging from −2 kb to TSS. CGI positions were obtained from UCSC (downloaded on 2 March 2017), and shores were defined as regions surrounding CGIs by up to 2 kb. All windows were annotated by comparing the window center genomic position with the positions of the aforementioned features with bedtools annotate. For visualization, sequencing tracks were uploaded as WIG files onto the UCSC genome browser. Read densities shown in the different figures were normalized to the total number of reads and expressed as $\log_2$ CPM.

Infinium Human Methylation 450K

Genomic DNA (300 to 800 ng) was converted with sodium bisulfite using the Zymo EZ DNA Methylation Kit (Zymo Research). Methylation assays were performed with 4 ml of converted DNA at 50 ng/ml, according to the manufacturer's protocol. Infinium Human Methylation 450K raw data were submitted to the GEO database (GSE101445).

Raw Infinium data were filtered by removing low-quality data using a detection P value threshold of 0.05. Cross-reactive and single-nucleotide polymorphism–containing probes were filtered out using the extended annotation provided by Price *et al.* (*81*). β values were computed with the formula: $\beta\ \text{value} = M/[U + M]$, where M and U are the raw "methylated" and "unmethylated" signals, respectively. The β values were corrected for type I and type II bias by peak-based correction. Finally, the delta-β value was computed as the mean of the absolute difference between the tumor β value and the β value of the adjacent normal tissue.

Statistical analyses

Unless otherwise indicated, all experiments included technical replicates and were repeated at least three independent times. Data and graphs are presented as averages ± SDs. Data were compared by means of two-tailed t tests. When more than two groups were compared, one-way ANOVA analyses were performed. The statistical significance criterion was $P \leq 0.05$. $^{*}P \leq 0.05$, $^{**}P \leq 0.01$, and $^{***}P \leq 0.001$.

SUPPLEMENTARY MATERIALS

Supplementary material for this article is available at http://advances.sciencemag.org/cgi/content/full/4/6/eaap7309/DC1

fig. S1. Characterization of BC samples used in genome-wide analyses.
fig. S2. *TET1* and immune markers in non-BLBC BC subtypes.
fig. S3. *TET1* expression and immunity in BLBC.
fig. S4. Non-BLBC subtypes do not show a strong correlation between *TET1* expression and immunity.
fig. S5. Immune pathways modulate *TET1* expression in BC.
fig. S6. Activation of NF-κB in BC cells.
fig. S7. NF-κB and TET1 in additional BC cell lines.
fig. S8. Immunity and TET2 and TET3 in BLBC.
fig. S9. *TET1* promoter and streptavidin-agarose pulldown probes.
fig. S10. *TET1* and immunity in thyroid, melanoma, and lung cancers.
fig. S11. *TET1* and immunity in additional cancer types.
fig. S12. *TET1* expression and NF-κB in additional cancer types.
table S1. List of dhmRs in BLBC (Excel file).
table S2. Genes negatively correlating with TET1 in BLBC (TCGA)—Top 5 of gene ontology categories.
table S3. Genes positively correlating with TET1 in BLBC (TCGA)—Top 5 of gene ontology categories.
table S4. List of primers.

REFERENCES AND NOTES

1. A. G. Rivenbark, S. M. O'Connor, W. B. Coleman, Molecular and cellular heterogeneity in breast cancer: Challenges for personalized medicine. *Am. J. Pathol.* **183**, 1113–1124 (2013).
2. C. M. Perou, T. Sørlie, M. B. Eisen, M. van de Rijn, S. S. Jeffrey, C. A. Rees, J. R. Pollack, D. T. Ross, H. Johnsen, L. A. Akslen, Ø. Fluge, A. Pergamenschikov, C. Williams, S. X. Zhu, P. E. Lønning, A.-L. Børresen-Dale, P. O. Brown, D. Botstein, Molecular portraits of human breast tumours. *Nature* **406**, 747–752 (2000).
3. T. Sørlie, C. M. Perou, R. Tibshirani, T. Aas, S. Geisler, H. Johnsen, T. Hastie, M. B. Eisen, M. van de Rijn, S. S. Jeffrey, T. Thorsen, H. Quist, J. C. Matese, P. O. Brown, D. Botstein, P. E. Lønning, A.-L. Børresen-Dale, Gene expression patterns of breast carcinomas distinguish tumor subclasses with clinical implications. *Proc. Natl. Acad. Sci. U.S.A.* **98**, 10869–10874 (2001).
4. C. Sotiriou, S.-Y. Neo, L. M. McShane, E. L. Korn, P. M. Long, A. Jazaeri, P. Martiat, S. B. Fox, A. L. Harris, E. T. Liu, Breast cancer classification and prognosis based on

gene expression profiles from a population-based study. *Proc. Natl. Acad. Sci. U.S.A.* **100**, 10393–10398 (2003).
5. T. Sørlie, R. Tibshirani, J. Parker, T. Hastie, J. S. Marron, A. Nobel, S. Deng, H. Johnsen, R. Pesich, S. Geisler, J. Demeter, C. M. Perou, P. E. Lønning, P. O. Brown, A.-L. Børresen-Dale, D. Botstein, Repeated observation of breast tumor subtypes in independent gene expression data sets. *Proc. Natl. Acad. Sci. U.S.A.* **100**, 8418–8423 (2003).
6. N. P. Tobin, J. C. Harrell, J. Lövrot, S. Egyhazi Brage, M. Frostvik Stolt, L. Carlsson, Z. Einbeigi, B. Linderholm, N. Loman, M. Malmberg, T. Walz, M. Fernö, C. M. Perou, J. Bergh, T. Hatschek, L. S. Lindström; TEX Trialists Group, Molecular subtype and tumor characteristics of breast cancer metastases as assessed by gene expression significantly influence patient post-relapse survival. *Ann. Oncol.* **26**, 81–88 (2015).
7. M. Berdasco, M. Esteller, Aberrant epigenetic landscape in cancer: How cellular identity goes awry. *Dev. Cell* **19**, 698–711 (2010).
8. R. B. Lorsbach, J. Moore, S. Mathew, S. C. Raimondi, S. T. Mukatira, J. R. Downing, TET1, a member of a novel protein family, is fused to MLL in acute myeloid leukemia containing the t(10;11)(q22;q23). *Leukemia* **17**, 637–641 (2003).
9. M. Münzel, D. Globisch, T. Carell, 5-Hydroxymethylcytosine, the sixth base of the genome. *Angew. Chem. Int. Ed. Engl.* **50**, 6460–6468 (2011).
10. M. Tahiliani, K. P. Koh, Y. Shen, W. A. Pastor, H. Bandukwala, Y. Brudno, S. Agarwal, L. M. Iyer, D. R. Liu, L. Aravind, A. Rao, Conversion of 5-methylcytosine to 5-hydroxymethylcytosine in mammalian DNA by MLL partner TET1. *Science* **324**, 930–935 (2009).
11. S. Ito, A. C. D'Alessio, O. V. Taranova, K. Hong, L. C. Sowers, Y. Zhang, Role of Tet proteins in 5mC to 5hmC conversion, ES-cell self-renewal and inner cell mass specification. *Nature* **466**, 1129–1133 (2010).
12. L. Li, C. Li, H. Mao, Z. Du, W. Y. Chan, P. Murray, B. Luo, A. T. Chan, T. S. Mok, F. K. Chan, R. F. Ambinder, Q. Tao, Epigenetic inactivation of the CpG demethylase TET1 as a DNA methylation feedback loop in human cancers. *Sci. Rep.* **6**, 26591 (2016).
13. Y. Xu, F. Wu, L. Tan, L. Kong, L. Xiong, J. Deng, A. Barbera, L. Zheng, H. Zhang, S. Huang, J. Min, T. Nicholson, T. Chen, G. Xu, Y. Shi, K. Zhang, Y. G. Shi, Genome-wide regulation of 5hmC, 5mC, and gene expression by Tet1 hydroxylase in mouse embryonic stem cells. *Mol. Cell* **42**, 451–464 (2011).
14. J. U. Guo, Y. Su, C. Zhong, G.-l. Ming, H. Song, Hydroxylation of 5-methylcytosine by TET1 promotes active DNA demethylation in the adult brain. *Cell* **145**, 423–434 (2011).
15. W. A. Pastor, L. Aravind, A. Rao, TETonic shift: Biological roles of TET proteins in DNA demethylation and transcription. *Nat. Rev. Mol. Cell Biol.* **14**, 341–356 (2013).
16. M. C. Haffner, A. Chaux, A. K. Meeker, D. M. Esopi, J. Gerber, L. G. Pellakuru, A. Toubaji, P. Argani, C. Iacobuzio-Donahue, W. G. Nelson, G. J. Netto, A. M. De Marzo, S. Yegnasubramanian, Global 5-hydroxymethylcytosine content is significantly reduced in tissue stem/progenitor cell compartments and in human cancers. *Oncotarget* **2**, 627–637 (2011).
17. C. G. Lian, Y. Xu, C. Ceol, F. Wu, A. Larson, K. Dresser, W. Xu, L. Tan, Y. Hu, Q. Zhan, C.-w. Lee, D. Hu, B. Q. Lian, S. Kleffel, Y. Yang, J. Neiswender, A. J. Khorasani, R. Fang, C. Lezcano, L. M. Duncan, R. A. Scolyer, J. F. Thompson, H. Kakavand, Y. Houvras, L. Zon, M. C. Mihm Jr., U. B. Kaiser, T. Schatton, B. A. Woda, G. F. Murphy, Y. G. Shi, Loss of 5-hydroxymethylcytosine is an epigenetic hallmark of melanoma. *Cell* **150**, 1135–1146 (2012).
18. C. H. Hsu, K. L. Peng, M. L. Kang, Y. R. Chen, Y. C. Yang, C. H. Tsai, C. S. Chu, Y. M. Jeng, Y. T. Chen, F. M. Lin, H. D. Huang, Y. Y. Lu, Y. C. Teng, S. T. Lin, R. K. Lin, F. M. Tang, S. B. Lee, H. M. Hsu, J. C. Yu, P. W. Hsiao, L. J. Juan, TET1 suppresses cancer invasion by activating the tissue inhibitors of metalloproteinases. *Cell Rep.* **2**, 568–579 (2012).
19. F. Neri, D. Dettori, D. Incarnato, A. Krepelova, S. Rapelli, M. Maldotti, C. Parlato, P. Paliogiannis, S. Oliviero, TET1 is a tumour suppressor that inhibits colon cancer growth by derepressing inhibitors of the WNT pathway. *Oncogene* **34**, 4168–4176 (2015).
20. L. Yang, S.-J. Yu, Q. Hong, Y. Yang, Z.-M. Shao, Reduced expression of TET1, TET2, TET3 and TDG mRNAs are associated with poor prognosis of patients with early breast cancer. *PLOS ONE* **10**, e0133896 (2015).
21. H.-G. Lu, W. Zhan, L. Yan, R.-Y. Qin, Y.-P. Yan, Z.-J. Yang, G.-C. Liu, G.-Q. Li, H.-F. Wang, X.-L. Li, Z. Li, L. Gao, G.-Q. Chen, TET1 partially mediates HDAC inhibitor-induced suppression of breast cancer invasion. *Mol. Med. Rep.* **10**, 2595–2600 (2014).
22. Y. Sang, C. Cheng, X.-F. Tang, M.-F. Zhang, X.-B. Lv, Hypermethylation of TET1 promoter is a new diagnosic marker for breast cancer metastasis. *Asian Pac. J. Cancer Prev.* **16**, 1197–1200 (2015).
23. Y.-f. Pei, Y. Lei, X.-q. Liu, MiR-29a promotes cell proliferation and EMT in breast cancer by targeting ten eleven translocation 1. *Biochim. Biophys. Acta* **1862**, 2177–2185 (2016).
24. M. Sun, C.-X. Song, H. Huang, C. A. Frankenberger, D. Sankarasharma, S. Gomes, P. Chen, J. Chen, K. K. Chada, C. He, M. R. Rosner, HMGA2/TET1/HOXA9 signaling pathway regulates breast cancer growth and metastasis. *Proc. Natl. Acad. Sci. U.S.A.* **110**, 9920–9925 (2013).
25. B. Lakshmi Narendra, K. Eshvendar Reddy, S. Shantikumar, S. Ramakrishna, Immune system: A double-edged sword in cancer. *Inflamm. Res.* **62**, 823–834 (2013).
26. B. Melichar, H. Študentová, H. Kalábová, D. Vitásková, P. Čermáková, H. Hornychová, A. Ryška, Predictive and prognostic significance of tumor-infiltrating lymphocytes in patients with breast cancer treated with neoadjuvant systemic therapy. *Anticancer Res.* **34**, 1115–1125 (2014).
27. D. A. Oble, R. Loewe, P. Yu, M. C. Mihm Jr., Focus on TILs: Prognostic significance of tumor infiltrating lymphocytes in human melanoma. *Cancer Immunol. Res.* **9**, 3 (2009).
28. J. Galon, A. Costes, F. Sanchez-Cabo, A. Kirilovsky, B. Mlecnik, C. Lagorce-Pagès, M. Tosolini, M. Camus, A. Berger, P. Wind, F. Zinzindohoué, P. Bruneval, P.-H. Cugnenc, Z. Trajanoski, W.-H. Fridman, F. Pagès, Type, density, and location of immune cells within human colorectal tumors predict clinical outcome. *Science* **313**, 1960–1964 (2006).
29. M. Dany, R. Nganga, A. Chidiac, E. Hanna, S. Matar, D. Elston, Advances in immunotherapy for melanoma management. *Hum. Vaccines Immunother.* **12**, 2501–2511 (2016).
30. S. Gerondakis, U. Siebenlist, Roles of the NF-κB pathway in lymphocyte development and function. *Cold Spring Harb. Perspect. Biol.* **2**, a000182 (2010).
31. A. Hoffmann, D. Baltimore, Circuitry of nuclear factor κB signaling. *Immunol. Rev.* **210**, 171–186 (2006).
32. A. Oeckinghaus, S. Ghosh, The NF-κB family of transcription factors and its regulation. *Cold Spring Harb. Perspect. Biol.* **1**, a000034 (2009).
33. B. P. Ashburner, S. D. Westerheide, A. S. Baldwin Jr., The p65 (RelA) subunit of NF-κB interacts with the histone deacetylase (HDAC) corepressors HDAC1 and HDAC2 to negatively regulate gene expression. *Mol. Cell. Biol.* **21**, 7065–7077 (2001).
34. S. I. Grivennikov, F. R. Greten, M. Karin, Immunity, inflammation, and cancer. *Cell* **140**, 883–899 (2010).
35. B. Hoesel, J. A. Schmid, The complexity of NF-κB signaling in inflammation and cancer. *Mol. Cancer* **12**, 86 (2013).
36. A. Mantovani, Molecular pathways linking inflammation and cancer. *Curr. Mol. Med.* **10**, 369–373 (2010).
37. D. M. Brantley, C.-L. Chen, R. S. Muraoka, P. B. Bushdid, J. L. Bradberry, F. Kittrell, D. Medina, L. M. Matrisian, L. D. Kerr, F. E. Yull, Nuclear factor-κB (NF-κB) regulates proliferation and branching in mouse mammary epithelium. *Mol. Biol. Cell* **12**, 1445–1455 (2001).
38. N. Yamaguchi, T. Ito, S. Azuma, E. Ito, R. Honma, Y. Yanagisawa, A. Nishikawa, M. Kawamura, J.-i. Imai, S. Watanabe, K. Semba, J.-i. Inoue, Constitutive activation of nuclear factor-κB is preferentially involved in the proliferation of basal-like subtype breast cancer cell lines. *Cancer Sci.* **100**, 1668–1674 (2009).
39. M. Liu, T. Sakamaki, M. C. Casimiro, N. E. Willmarth, A. A. Quong, X. Ju, J. Ojeifo, X. Jiao, W.-S. Yeow, S. Katiyar, L. A. Shirley, D. Joyce, M. P. Lisanti, C. Albanese, R. G. Pestell, The canonical NF-κB pathway governs mammary tumorigenesis in transgenic mice and tumor stem cell expansion. *Cancer Res.* **70**, 10464–10473 (2010).
40. L. Connelly, W. Barham, H. M. Onishko, T. Sherrill, L. A. Chodosh, T. S. Blackwell, F. E. Yull, Inhibition of NF-kappa B activity in mammary epithelium increases tumor latency and decreases tumor burden. *Oncogene* **30**, 1402–1412 (2011).
41. M. Karin, Nuclear factor-κB in cancer development and progression. *Nature* **441**, 431–436 (2006).
42. H. L. Chua, P. Bhat-Nakshatri, S. E. Clare, A. Morimiya, S. Badve, H. Nakshatri, NF-κB represses E-cadherin expression and enhances epithelial to mesenchymal transition of mammary epithelial cells: Potential involvement of ZEB-1 and ZEB-2. *Oncogene* **26**, 711–724 (2007).
43. W. E. Naugler, M. Karin, NF-κB and cancer—Identifying targets and mechanisms. *Curr. Opin. Genet. Dev.* **18**, 19–26 (2008).
44. D. Joyce, C. Albanese, J. Steer, M. Fu, B. Bouzahzah, R. G. Pestell, NF-κB and cell-cycle regulation: The cyclin connection. *Cytokine Growth Factor Rev.* **12**, 73–90 (2001).
45. S. A. Vlahopoulos, O. Cen, N. Hengen, J. Agan, M. Moschovi, E. Critselis, M. Adamaki, F. Bacopoulou, J. A. Copland, I. Boldogh, M. Karin, G. P. Chrousos, Dynamic aberrant NF-κB spurs tumorigenesis: A new model encompassing the microenvironment. *Cytokine Growth Factor Rev.* **26**, 389–403 (2015).
46. J. Y. Zhang, S. Tao, R. Kimmel, P. A. Khavari, CDK4 regulation by TNFR1 and JNK is required for NF-κB–mediated epidermal growth control. *J. Cell Biol.* **168**, 561–566 (2005).
47. S. Maeda, H. Kamata, J.-L. Luo, H. Leffert, M. Karin, IKKβ couples hepatocyte death to cytokine-driven compensatory proliferation that promotes chemical hepatocarcinogenesis. *Cell* **121**, 977–990 (2005).
48. W. Shibata, S. Takaishi, S. Muthupalani, D. M. Pritchard, M. T. Whary, A. B. Rogers, J. G. Fox, K. S. Betz, K. H. Kaestner, M. Karin, T. C. Wang, Conditional deletion of IκB-kinase-β accelerates *Helicobacter*-dependent gastric apoptosis, proliferation, and preneoplasia. *Gastroenterology* **138**, 1022–1034.e10 (2010).
49. D. Capece, D. Verzella, A. Tessitore, E. Alesse, C. Capalbo, F. Zazzeroni, Cancer secretome and inflammation: The bright and the dark sides of NF-κB. *Semin. Cell Dev. Biol.* **78**, 51–61 (2018).
50. S. Dedeurwaerder, C. Desmedt, E. Calonne, S. K. Singhal, B. Haibe-Kains, M. Defrance, S. Michiels, M. Volkmar, R. Deplus, J. Luciani, F. Lallemand, D. Larsimont, J. Toussaint, S. Haussy, F. Rothé, G. Rouas, O. Metzger, S. Majjaj, K. Saini, P. Putmans, G. Hames, N. van Baren, P. G. Coulie, M. Piccart, C. Sotiriou, F. Fuks, DNA methylation profiling reveals a predominant immune component in breast cancers. *EMBO Mol. Med.* **3**, 726–741 (2011).

51. K. B. Chiappinelli, P. L. Strissel, A. Desrichard, H. Li, C. Henke, B. Akman, A. Hein, N. S. Rote, L. M. Cope, A. Snyder, V. Makarov, S. Buhu, D. J. Slamon, J. D. Wolchok, D. M. Pardoll, M. W. Beckmann, C. A. Zahnow, T. Merghoub, T. A. Chan, S. B. Baylin, R. Strick, Inhibiting DNA methylation causes an interferon response in cancer via dsRNA including endogenous retroviruses. *Cell* **162**, 974–986 (2015).
52. D. Roulois, H. L. Yau, R. Singhania, Y. Wang, A. Danesh, S. Y. Shen, H. Han, G. Liang, P. A. Jones, T. J. Pugh, C. O'Brien, D. D. De Carvalho, DNA-demethylating agents target colorectal cancer cells by inducing viral mimicry by endogenous transcripts. *Cell* **162**, 961–973 (2015).
53. K. B. Chiappinelli, C. A. Zahnow, N. Ahuja, S. B. Baylin, Combining epigenetic and immunotherapy to combat cancer. *Cancer Res.* **76**, 1683–1689 (2016).
54. Q. Zhang, K. Zhao, Q. Shen, Y. Han, Y. Gu, X. Li, D. Zhao, Y. Liu, C. Wang, X. Zhang, X. Su, J. Liu, W. Ge, R. L. Levine, N. Li, X. Cao, Tet2 is required to resolve inflammation by recruiting Hdac2 to specifically repress IL-6. *Nature* **525**, 389–393 (2015).
55. K. Ichiyama, T. Chen, X. Wang, X. Yan, B.-S. Kim, S. Tanaka, D. Ndiaye-Lobry, Y. Deng, Y. Zou, P. Zheng, Q. Tian, I. Aifantis, L. Wei, C. Dong, The methylcytosine dioxygenase Tet2 promotes DNA demethylation and activation of cytokine gene expression in T cells. *Immunity* **42**, 613–626 (2015).
56. S. A. Carty, M. Gohil, L. B. Banks, R. M. Cotton, M. E. Johnson, E. Stelekati, A. D. Wells, E. J. Wherry, G. A. Koretzky, M. S. Jordan, The loss of TET2 promotes $CD8^+$ T cell memory differentiation. *J. Immunol.* **200**, 82–91 (2018).
57. C. Yang, Z. Li, W. Kang, Y. Tian, Y. Yan, W. Chen, TET1 and TET3 are essential in induction of Th2-type immunity partly through regulation of IL-4/13A expression in zebrafish model. *Gene* **591**, 201–208 (2016).
58. B. Delatte, J. Jeschke, M. Defrance, M. Bachman, C. Creppe, E. Calonne, M. Bizet, R. Deplus, L. Marroquí, M. Libin, M. Ravichandran, F. Mascart, D. L. Eizirik, A. Murrell, T. P. Jurkowski, F. Fuks, Genome-wide hydroxymethylcytosine pattern changes in response to oxidative stress. *Sci. Rep.* **5**, 12714 (2015).
59. J. Jeschke, M. Bizet, C. Desmedt, E. Calonne, S. Dedeurwaerder, S. Garaud, A. Koch, D. Larsimont, R. Salgado, G. Van den Eynden, K. W. Gallo, G. Bontempi, M. Defrance, C. Sotiriou, F. Fuks, DNA methylation–based immune response signature improves patient diagnosis in multiple cancers. *J. Clin. Invest.* **127**, 3090–3102 (2017).
60. C. E. Hellweg, A. Arenz, S. Bogner, C. Schmitz, C. Baumstark-Khan, Activation of nuclear factor κB by different agents: Influence of culture conditions in a cell-based assay. *Ann. N. Y. Acad. Sci.* **1091**, 191–204 (2006).
61. D. H. Lee, A. L. Goldberg, Proteasome inhibitors: Valuable new tools for cell biologists. *Trends Cell Biol.* **8**, 397–403 (1998).
62. W. Barham, L. Chen, O. Tikhomirov, H. Onishko, L. Gleaves, T. P. Stricker, T. S. Blackwell, F. E. Yull, Aberrant activation of NF-κB signaling in mammary epithelium leads to abnormal growth and ductal carcinoma in situ. *BMC Cancer* **15**, 647 (2015).
63. H. Jókai, M. Marschalkó, J. Csomor, J. Szakonyi, O. Kontár, G. Barna, S. Kárpáti, P. Holló, Tissue-specific homing of immune cells in malignant skin tumors. *Pathol. Oncol. Res.* **18**, 749–759 (2012).
64. S. Imam, R. Paparodis, D. Sharma, J. C. Jaume, Lymphocytic profiling in thyroid cancer provides clues for failure of tumor immunity. *Endocr. Relat. Cancer* **21**, 505–516 (2014).
65. J. Kargl, S. E. Busch, G. H. Y. Yang, K.-H. Kim, M. L. Hanke, H. E. Metz, J. J. Hubbard, S. M. Lee, D. K. Madtes, M. W. McIntosh, A. M. Houghton, Neutrophils dominate the immune cell composition in non-small cell lung cancer. *Nat. Commun.* **8**, 14381 (2017).
66. Y. Kudo, K. Tateishi, K. Yamamoto, S. Yamamoto, Y. Asaoka, H. Ijichi, G. Nagae, H. Yoshida, H. Aburatani, K. Koike, Loss of 5-hydroxymethylcytosine is accompanied with malignant cellular transformation. *Cancer Sci.* **103**, 670–676 (2012).
67. B. Thienpont, J. Steinbacher, H. Zhao, F. D'Anna, A. Kuchnio, A. Ploumakis, B. Ghesquière, L. Van Dyck, B. Boeckx, L. Schoonjans, E. Hermans, F. Amant, V. N. Kristensen, K. P. Koh, M. Mazzone, M. L. Coleman, T. Carell, P. Carmeliet, D. Lambrechts, Tumour hypoxia causes DNA hypermethylation by reducing TET activity. *Nature* **537**, 63–68 (2016).
68. A. Sica, A. Mantovani, Macrophage plasticity and polarization: In vivo veritas. *J. Clin. Invest.* **122**, 787–795 (2012).
69. A. Mantovani, A. Sica, S. Sozzani, P. Allavena, A. Vecchi, M. Locati, The chemokine system in diverse forms of macrophage activation and polarization. *Trends Immunol.* **25**, 677–686 (2004).
70. F. Chen, K. Beezhold, V. Castranova, Tumor promoting or tumor suppressing of NF-κ B, a matter of cell context dependency. *Int. Rev. Immunol.* **27**, 183–204 (2008).
71. Y. Liu, M. W. Mayo, A. S. Nagji, P. W. Smith, C. S. Ramsey, D. Li, D. R. Jones, Phosphorylation of RelA/p65 promotes DNMT-1 recruitment to chromatin and represses transcription of the tumor metastasis suppressor gene *BRMS1*. *Oncogene* **31**, 1143–1154 (2012).
72. R. Yang, C. Qu, Y. Zhou, J. E. Konkel, S. Shi, Y. Liu, C. Chen, S. Liu, D. Liu, Y. Chen, E. Zandi, W. Chen, Y. Zhou, S. Shi, Hydrogen sulfide promotes Tet1- and Tet2-mediated *Foxp3* demethylation to drive regulatory T cell differentiation and maintain immune homeostasis. *Immunity* **43**, 251–263 (2015).
73. D. W. Huang, B. T. Sherman, R. A. Lempicki, Systematic and integrative analysis of large gene lists using DAVID bioinformatics resources. *Nat. Protoc.* **4**, 44–57 (2009).
74. A. M. Newman, C. L. Liu, M. R. Green, A. J. Gentles, W. Feng, Y. Xu, C. D. Hoang, M. Diehn, A. A. Alizadeh, Robust enumeration of cell subsets from tissue expression profiles. *Nat. Methods* **12**, 453–457 (2015).
75. S. J. Van Laere, I. Van der Auwera, G. G. Van den Eynden, H. J. Elst, J. Weyler, A. L. Harris, P. van Dam, E. A. Van Marck, P. B. Vermeulen, L. Y. Dirix, Nuclear factor-κB signature of inflammatory breast cancer by cDNA microarray validated by quantitative real-time reverse transcription-PCR, immunohistochemistry, and nuclear factor-κB DNA-binding. *Clin. Cancer Res.* **12**, 3249–3256 (2006).
76. M. M. Mohamed, Monocytes conditioned media stimulate fibronectin expression and spreading of inflammatory breast cancer cells in three-dimensional culture: A mechanism mediated by IL-8 signaling pathway. *Cell Commun. Signal* **10**, 3 (2012).
77. H. B. Sadowski, M. Z. Gilman, Cell-free activation of a DNA-binding protein by epidermal growth factor. *Nature* **362**, 79–83 (1993).
78. W.-G. Deng, Y. Zhu, A. Montero, K. K. Wu, Quantitative analysis of binding of transcription factor complex to biotinylated DNA probe by a streptavidin–agarose pulldown assay. *Anal. Biochem.* **323**, 12–18 (2003).
79. L. Buisseret, C. Desmedt, S. Garaud, M. Fornili, X. Wang, G. Vanden Eyden, A. de Wind, S. Duquenne, A. Boisson, C. Naveaux, F. Rothé, S. Rorive, C. Decaestecker, D. Larsimont, M. Piccart-Gebhart, E. Biganzoli, C. Sotiriou, K. Willard-Gallo, Reliability of tumor-infiltrating lymphocyte and tertiary lymphoid structure assessment in human breast cancer. *Mod. Pathol.* **30**, 1204–1212 (2017).
80. O. Van Grembergen, M. Bizet, E. J. de Bony, E. Calonne, P. Putmans, S. Brohée, C. Olsen, M. Guo, G. Bontempi, C. Sotiriou, M. Defrance, F. Fuks, Portraying breast cancers with long noncoding RNAs. *Sci. Adv.* **2**, e1600220 (2016).
81. E. M. Price, A. M. Cotton, L. L. Lam, P. Farré, E. Emberly, C. J. Brown, W. P. Robinson, M. S. Kobor, Additional annotation enhances potential for biologically-relevant analysis of the Illumina Infinium HumanMethylation450 BeadChip array. *Epigenetics Chromatin* **6**, 4 (2013).

Acknowledgments: We thank J. Jeschke for continued support and advice. E. Collignon was supported by a L'Oreal "For Women In Science" fellowship and by the Belgian "Fonds de la Recherche Scientifique" (FNRS). A.C., M.B., and C.A.W. were supported by Télévie grants. A.C. was also supported by the "Fondation Léon Fredericq." F.F. is a ULB Full Professor. F.F.'s laboratory was funded by grants from the FNRS and Télévie, the Interuniversity Attraction Poles (P7/03) program, the "Action de Recherche Concertée" (ARC) (AUWB-2010-2015 ULB-No 7), the Wallonie-Bruxelles Health program (CANDX 1318030), the Belgian "Fondation contre le Cancer" (FCC 2016-086 FAF-F/2016/872), and the Fonds Gaston Ithier. A.N.'s laboratory was supported by Belgian grants from the Belgian FNRS, Télévie, the "Centre Anti-Cancéreux," the Fondation Léon Fredericq, and the "Fonds Spéciaux" of the University of Liège. K.W.-G.'s laboratory is supported by grants from the Belgian FNRS, Les Amis de l'Institut Bordet, Télévie, Plan Cancer of Belgium, MEDIC Foundation, and Fondation Lambeau-Marteaux. F.Y.'s laboratory was supported by NIH R01 CA214043. **Author contributions:** E. Collignon and A.C. designed and conducted the experiments and interpreted data. C.A.W. performed streptavidin-agarose pulldown assays and Western blotting. W.B., A.W., and F.Y. prepared and collected mouse samples. C.S. collected human breast biopsies. E. Calonne performed genome-wide mapping of 5hmC and 5mC. E. Collignon, M.B., and S.D. conducted bioinformatic and statistical analyses. S.G., C.N., and K.W.-G. performed IHC analyses. P.H. prepared macrophage-conditioned medium. S.B. and C.V.L. identified consensus binding sequences and helped to design NF-κB activation and binding experiments. F.F. and A.N. designed experiments, interpreted data, and supervised the study. E. Collignon, A.C., F.F., and A.N. wrote the manuscript. **Competing interests:** C.V.L. is a Research Director of the FNRS (Belgium). The other authors declare that they have no competing interests. **Data and materials availability:** All data needed to evaluate the conclusions in the paper are present in the paper and/or the Supplementary Materials. Additional data related to this paper may be requested from the authors.

Submitted 13 October 2017
Accepted 9 May 2018
Published 20 June 2018
10.1126/sciadv.aap7309

Citation: E. Collignon, A. Canale, C. Al Wardi, M. Bizet, E. Calonne, S. Dedeurwaerder, S. Garaud, C. Naveaux, W. Barham, A. Wilson, S. Bouchat, P. Hubert, C. Van Lint, F. Yull, C. Sotiriou, K. Willard-Gallo, A. Noel, F. Fuks, Immunity drives *TET1* regulation in cancer through NF-κB. *Sci. Adv.* **4**, eaap7309 (2018).